AD-A045 620 FRANK J SEILER RESEARCH LAB UNITED STATES AIR FORCE --ETC F/G 10/3
THE DISCHARGE BEHAVIOR OF A LIAL/NAALCL4/CUCL2 PELLETIZED THERM--ETC(U)
FEB 77 J K ERBACHER, C L HUSSEY, L A KING
UNCLASSIFIED FJSRL-TR-77-0001 NL

1 OF 2
ADA045 620

~~END~~ CONT.
DATE
FILMED
11-77
DDC

1 OF 2

ADA045620

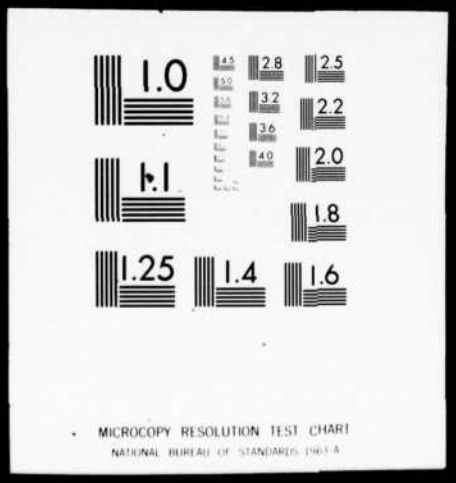

(12)

FRANK J. SEILER RESEARCH LABORATORY

FJSRL TECHNICAL REPORT-77-0001

FEBRUARY 1977

THE DISCHARGE BEHAVIOR OF A $LiAl/NaAlCl_4/CoCl_2$ PELLETIZED THERMAL CELL

PROJECT 2303

AIR FORCE SYSTEMS COMMAND

UNITED STATES AIR FORCE

NOTICE

When Government drawings, specifications, or other data are used for any purpose other than in connection with a definitely related Government procurement operation, the United States Government thereby incurs no responsibility nor any obligation whatsoever; and the fact that the Government may have formulated, furnished, or in any way supplied the said drawings, specifications, or other data, is not to be regarded by implication or otherwise as in any manner licensing the holder or any other person or corporation, or conveying any rights or permission to manufacture, use, or sell any patented invention that may in any way be related thereto.

Inquiries concerning this document should be addressed to the Frank J. Seiler Research Laboratory (FJSRL/NC), US Air Force Academy, Colorado 80840 (telephone 303/472-2655).

Copies of this report should not be returned unless return is required by security considerations, contractual obligations, or notice on a specific document.

Printed in the United States of America
Available from
National Technical Information Service
U.S. Department of Commerce
5285 Port Royal Road
Springfield, Virginia 22151

Unclassified

SECURITY CLASSIFICATION OF THIS PAGE (When Data Entered)

REPORT DOCUMENTATION PAGE

READ INSTRUCTIONS BEFORE COMPLETING FORM

1. REPORT NUMBER: FJSRL-TR-77-0001
2. GOVT ACCESSION NO.: ADA-
3. RECIPIENT'S CATALOG NUMBER:
4. TITLE (and Subtitle): The Discharge Behavior of a $LiAl/NaAlCl_4/CuCl_2$ Pelletized Thermal Cell
5. TYPE OF REPORT & PERIOD COVERED: Technical Report, Jan 1976 - Feb 1977
6. PERFORMING ORG. REPORT NUMBER:
7. AUTHOR(s): Capt John K. Erbacher, Capt Charles L. Hussey, Lt Col Lowell A. King
8. CONTRACT OR GRANT NUMBER(s):
9. PERFORMING ORGANIZATION NAME AND ADDRESS: F. J. Seiler Research Laboratory (AFSC), FJSRL/NC, U. S. Air Force Academy, Colorado 80840
10. PROGRAM ELEMENT, PROJECT, TASK AREA & WORK UNIT NUMBERS: New 61102F/2303/F2/07; Old 61102/7903/02/07
11. CONTROLLING OFFICE NAME AND ADDRESS: F. J. Seiler Research Laboratory (AFSC), FJSRL/NC, U. S. Air Force Academy, Colorado 80840
12. REPORT DATE: February 1977
13. NUMBER OF PAGES: 53
14. MONITORING AGENCY NAME & ADDRESS (if different from Controlling Office):
15. SECURITY CLASS. (of this report): Unclassified
15a. DECLASSIFICATION/DOWNGRADING SCHEDULE: N/A
16. DISTRIBUTION STATEMENT (of this Report): Approved for public release; distribution unlimited.

17. DISTRIBUTION STATEMENT (of the abstract entered in Block 20, if different from Report):
18. SUPPLEMENTARY NOTES

319 920

19. KEY WORDS (Continue on reverse side if necessary and identify by block number)

Thermal Battery
Aluminum Chloride
Copper(II) Chloride
Lithium-Aluminum Alloys
Tetrachloroaluminate
Reserve Battery
Single Cells

20. ABSTRACT (Continue on reverse side if necessary and identify by block number)

Pelletized thermal battery single cell experiments on the lithium-aluminum alloy/sodium tetrachloroaluminate/copper(II) chloride electrochemical system are described. The effects of copper(II) chloride particle size, brand of graphite in the cathode, variation of the Li content of the alloy anodes, current density, and discharge temperature under constant current discharge conditions are discussed. A mechanism for the reaction of LiAl alloys in the $NaAlCl_4$ electrolyte is proposed.

DD FORM 1 JAN 73 1473 EDITION OF 1 NOV 65 IS OBSOLETE

Unclassified

SECURITY CLASSIFICATION OF THIS PAGE (When Data Entered)

THE DISCHARGE BEHAVIOR OF A

$LiAl/NaAlCl_4/CuCl_2$ PELLETIZED THERMAL CELL

John K. Erbacher
Charles L. Hussey
Lowell A. King

Technical Report SRL-TR-77-0001

February 1977

Director of Chemical Sciences
Frank J. Seiler Research Laboratory
Air Force Systems Command
US Air Force Academy, Colorado 80840

FOREWORD

This report was prepared by the Directorate of Chemical Sciences, Frank J. Seiler Research Laboratory, United States Air Force Academy, Colorado. The work was initiated under Project No. 2303, "Chemistry," Task No. 2303-F2, "Physical Chemistry and Electrochemistry," Work Unit No. 2303-F2-07, "Pelletized Thermal Batteries."

The report covers work conducted from January 1976 to February 1977. The manuscript was released by the authors for publication in February 1977.

The authors wish to acknowledge the assistance they received from Professor R.A. Osteryoung of Colorado State University, Fort Collins, Colorado; from D.M. Bush, A.R. Baldwin, and B.H. Van Domelen of Sandia Laboratories, Albuquerque, New Mexico; and from W.S. Bishop of the Air Force Aeropropulsion Laboratory, Wright-Patterson AFB, Ohio.

This technical report has been reviewed and approved.

BEN A. LOVING, LtCol, USAF
Director, Directorate of Chemical Sciences

TABLE OF CONTENTS

Section	Page
INTRODUCTION	1
EXPERIMENTAL	5
The Inert Atmosphere System	5
Electrolyte Materials	5
Cathode and Anode Materials	5
Current Collectors	7
Electrolyte Preparation	7
Pellet Fabrication	7
The Single Cell Discharge System	7
RESULTS AND DISCUSSION	12
Error Analysis	12
Graphite Studies	13
Copper(II) Chloride Particle Size	16
Aluminum, Lithium, and Lithium Aluminum Alloy Anodes	21
Current Density	29
Temperature Effects	32
CONCLUSIONS	41
REFERENCES	43
APPENDICES	
A - Basic Program: Constant Current Discharge	47
B - Abbreviated Sample Output: Constant Current Discharge Program	50
C - Energy Density Calculations	52
D - Coulombic Efficiency Calculations	54

LIST OF FIGURES

Figure		Page
1	Typical Cell Configuration Between Heated Platens	8
2	Platen Press Single Cell Tester - Model 2	10
3	Discharge Behavior as a Function of Different Graphites at 3.95 mA/cm^2 and 175°C	15
4	Discharge Behavior as a Function of Graphite Content at 15.0 mA/cm^2 and 200°C	18
5	Discharge Behavior as a Function of Different Anodes at 15.0 mA/cm^2 and 175°C for	
	5A - Li Dispersion, 90.9 a/o LiAl Alloy, Al Sheet, and Al Powder	23
	5B - 90.9, 70.4, 60.2, and 48.0 a/o LiAl Alloys	24
6	Voltage-Time Curves During Temperature Activation for (A) $Al/NaAlCl_4/CuCl_2$ Single Cell, (B) LiAl (48.0 a/o)/ $NaAlCl_4/CuCl_2$ Single Cell, and (C) $Li/NaAlCl_4/CuCl_2$ Single Cell	25
7	Energy Density to 80% of the ICCV as a Function of Discharge Rate at 175°C	31
8	Closed Circuit Voltage as a Function of Current for a LiAl(48.0 a/o)/$NaAlCl_4/CuCl_2$ Single Cell at 175°C	34
9	Open Circuit Voltage of a LiAl(48.0 a/o)/$NaAlCl_4/CuCl_2$ Single Cell as a Function of Temperature	37
10	Energy Densities as a Function of Temperature	39

LIST OF TABLES

Table		Page
I	Single Cell Pellet Composition and Compaction Pressures	9
II	Discharge Behavior as a Function of Different Graphites at 3.95 mA/cm^2 and 175°C	14
III	Discharge Behavior as a Function of Graphite Content at 15.0 mA/cm^2 and 200°C	17
IV	Discharge Behavior as a Function of $CuCl_2$ Particle Size	20
V	Discharge Behavior as a Function of Different Anodes at 15.0 mA/cm^2 and 175°C	22
VI	Discharge Behavior as a Function of Current Density at 175°C	30
VII	Cell Resistance as a Function of Extent of Discharge at 96.3 mA and 175°C	33
VIII	Open Circuit Voltages as a Function of Temperature	36
IX	Discharge Behavior as a Function of Temperature at 15.0 mA/cm^2	38

INTRODUCTION

Thermally activated galvanic cells have been of considerable interest in the aerospace field since World War II. Early cells utilized a "cup and cover" or similar design, which was followed in the 1950's by the development of a "pelletized" cell. Further development in pellet cell technology occurred gradually until Sandia Laboratories manufactured the first completely pelletized thermal battery for production use in 1966 (1). The interested reader is referred to the paper of Van Domelen and Wehrle (1) for the development of thermal battery technology and to Jennings (2) for a review of the various electrochemical systems currently utilized in thermal batteries.

General characteristics of current production thermal batteries include:

1. Utilization of a LiCl-KCl eutectic electrolyte.
2. An operational temperature range between 400° and 600°C.
3. A lifetime ranging from a few seconds to several minutes.

Recent work (3-7) at Sandia Laboratories has shown that current thermal battery systems can operate for as long as an hour under suitable conditions. This improvement in activated lifetime suggests thermal batteries are a potential power source for long life applications, including guided bombs, missiles, ECM devices, and torpedoes. A disadvantage of present systems for long life applications is the 400° to 600°C operating temperatures. The high operating temperature range necessitates heavier insulation to attain the extended lifetime and to prevent overheating of adjacent electronic components.

During recent years, problems have arisen with certain chemical

components required for thermal batteries (8). The health hazards associated with Cr(VI) compounds and shortages of some raw materials has led to renewed interest in alternate electrochemical couples for the present electrolyte system. Completely new electrolyte systems and couples for thermal battery applications are also desired. Several desirable characteristics for new systems are:

1. A lower operating temperature. This would reduce insulation requirements, battery volume, and conserve heat producing materials required for activation.

2. Avoidance of Cr(VI) compounds for the cathode. This would eliminate a primary carcinogenic health hazard.

Several electrolytes were investigated (9,10) to evaluate their applicability to low temperature thermal batteries. Mulligan (10) at Harry Diamond Laboratories, determined that a 70:30 m/o [mole %] KSCN-NaSCN electrolyte in conjunction with various lithium metal alloy anodes and a V_2O_5 cathode showed promise for high spin artillery shell applications. Krieger (11), also at Harry Diamond Laboratories, developed a heat reservoir to stabilize operational temperatures in the KSCN-NaSCN electrolyte system. Previous work at the Frank J. Seiler Research Laboratory has shown that a $NaAlCl_4$ electrolyte can be used with a variety of electrochemical couples in a pelletized thermal battery single cell configuration (12).

In the study conducted by Hussey, et al. (12), many single cells were evaluated for potential application to a new thermal battery system. One of the couples tested, which showed promise for long life applications, was the $Al/CuCl_2$ couple. This couple at a 3.95 mA/cm^2

constant current discharge rate and 175°C exhibited:

1. A stable open circuit voltage, 1.77 volts.
2. A high load voltage, 1.55 volts.
3. A long discharge lifetime, 100 minutes.
4. A sharp cutoff upon cell exhaustion.
5. A high open circuit voltage energy density, 261 W-Hr/lb.

Although the $CuCl_2$ cathode was not tested versus a LiAl alloy anode in that study, other cathodes were. Based on the evaluation of the other cathodes, it was expected that the open circuit and load voltages would be enhanced in a $LiAl/NaAlCl_4/CuCl_2$ cell. The previous results with an aluminum anode and the probable increases for a LiAl alloy anode, make the $CuCl_2$ cathode a candidate for a long life pelletized thermal battery system. Accordingly, a rather extensive evaluation of this cathode was initiated in January 1976 at this laboratory.

Copper(II) chloride is not a new cathode material. It has been utilized successfully for a number of years in bulk cells of the type Li or $LiAl/LiAlCl_4$-aprotic solvent/$CuCl_2$ (13-17). Copper(II) chloride was evaluated as a cathode for production thermal batteries by Levy and Reinhardt (18) in 1975. They compared $CuCl_2$ to $CaCrO_4$ in single cells of the type $Ca/LiCl\text{-}KCl/CaCrO_4$ from 400°-550°C at 60 mA/cm^2. The average peak voltage was 2.28V and the maximum cell lifetime to 80% of peak voltage was 4.95 minutes at 450°C. The performance of $CuCl_2$ single cells did not warrant additional study compared to other cathodes evaluated in that report. Senderoff's patent (19) claims $CuCl_2$ as a cathode in the system $LiAl/LiAlCl_4/CuCl_2$ but the open circuit voltage data reported do not correspond to that for the $LiAl/CuCl_2$

couple utilizing a $NaAlCl_4$ electrolyte observed in this laboratory (12) or by Boxall et al. (20). His data however, do agree very well with that observed for the Al/CuCl couple (20) and our own unpublished results for the LiAl/CuCl couple.

The basic electrochemistry of $CuCl_2$ in a $NaCl$-$AlCl_3$ electrolyte was studied using cyclic voltammetry, pulse polarography, and potentiometry by Boxall et al. (20). They determined that Cu(II) in a chloride-rich $NaAlCl_4$ melt at 175°C undergoes two reduction steps:

$$Cu(II) + e^- \rightleftharpoons Cu(I) \quad (1)$$

$$Cu(I) + e^- \rightleftharpoons Cu(0) \quad (2)$$

The first wave, at about 1.66V versus an Al reference electrode in the 1:1 melt (defined as 50:50 m/o $AlCl_3$:NaCl), is of primary importance in battery applications and appears to be a well behaved reversible electrochemical couple. The E° value reported for the Cu^{2+}/Cu^+ couple was 1.817 ± 0.005V at 175°C in the 1:1 melt. They also found that $CuCl_2$ was slightly soluble in that electrolyte, approximately 5 mM.

Studies conducted by this laboratory on LiAl/$NaAlCl_4$/$CuCl_2$ single cells included the effects of:

1. Different commercial graphites.
2. Catholyte graphite content.
3. $CuCl_2$ particle size.
4. LiAl alloy composition versus sheet and powdered Al.
5. Current density.
6. Temperature.

EXPERIMENTAL

The Inert Atmosphere System

Electrolyte preparation, cell fabrication, and single cell discharge experiments were conducted in either a nitrogen or argon filled Inert Atmosphere System (Vacuum/Atmospheres Co. Model HE-43-6 Dri-Lab/HE-493 Dri-Train). The moisture content was maintained below 15 PPM_V and the oxygen content was estimated to be 5 PPM_V using the 25 W lightbulb method of Foust (21). Initially all experiments were performed under a nitrogen atmosphere, but when lithium-alumium alloys were used as anodes the atmosphere was converted to argon to preclude formation of lithium nitrides and the associated lithium fire hazard.

Electrolyte Materials

Aluminum Chloride - Anhydrous iron free A.G. aluminum chloride was obtained from Fluka through Tridom Chemical Inc. and was used as received.

Sodium Chloride - "Baker Analyzed" reagent grade sodium chloride was used as received.

Binding Agent - Cab-O-Sil*, a high surface area fumed silicon dioxide was obtained from the Cabot Corporation and was dried at 400°C for one hour prior to use.

Cathode and Anode Materials

Copper(II) Chloride - Anhydrous copper(II) chloride (51.3% Cl equivalent to 98.6% $CuCl_2$) was obtained from Alfa-Ventron, Inc. in

---

*Registered Trade Mark, The Cabot Corporation

crude granular form. It was subsequently separated using standard ASTM sieves into <30, 30-50, 50-100, and >100 mesh sizes. In addition, a small quantity was ground in a CRC Micro-Mill* to pass through an ASTM 250 mesh sieve.

Graphite - Commercial graphites were obtained from Fisher Scientific Co. (Grade #38), Alfa-Ventron, Inc. (99.5% pure, 300 mesh), and Superior Graphite Co. (No. 1 large graphite flakes). The Superior graphite flakes were ground before use in a CRC Micro-Mill while the others were used as received. Half of the ground graphite flakes were also purified at 600°C under a chlorine atmosphere (9).

Aluminum - Sheet aluminum obtained from the Aluminum Corporation of America (99.5% pure, 0.0323 cm thick) was cut to 2.86 cm diameter circles, polished with emery cloth, rinsed with distilled water and acetone, and stored in the inert atmosphere system until needed. Powdered aluminum (99.9% pure, 100 mesh) was obtained from Research Organic/Inorganic Chemicals Co. and used as received.

Lithium-Aluminum Alloys - Lithium-aluminum alloys were obtained from Foote Mineral Co. (90.2 a/o lithium sheet, and 60 and 70 a/o lithium powder) and from Kawecki-Berylco Industries, Inc. (48 a/o lithium powder, 40-200 mesh) and stored under an argon atmosphere. The alloy powders were used as received. The alloy sheet was cut to a 2.86 cm diameter circle prior to use.

Lithium Metal Dispersion - A lithium metal dispersion sample (Foote Mineral Company Lot No. 208-1) was obtained through the courtesy of Mr Wayne S. Bishop (the Air Force Aeropropulsion Laboratory,

---

*Registered Trade Mark, The Chemical Rubber Co.

Wright-Patterson AFB, Ohio), stored under an argon atmosphere, and used as received.

Current Collectors

Nickel - Pure nickel sheet (0.0345 cm thick), obtained from Atlantic Equipment Engineers, was trimmed to the desired circle with tab and treated prior to use in the same manner as the sheet aluminum was treated. The current collectors were used repeatedly throughout the single cell experiments and were cleaned prior to each use.

Electrolyte Preparation

Aluminum chloride was fused with excess sodium chloride at 175°C and electrolytically purified for 24 hours utilizing a procedure developed by Boxall, et al. (20). Ten w/o [weight percent] Cab-O-Sil was combined with the molten $NaCl-AlCl_3$ mixture at 175°C to form a homogeneous paste, 10 w/o in the binder. The resulting Electrolyte Binder (EB) mixture was cooled, ground to a powder with a CRC Micro-Mill, and stored under an inert atmosphere.

Pellet Fabrication

Single cell pellets (Figure 1) were fabricated as described previously (12). Composition and compaction pressures are given in Table I. Bilayer pellets for use with sheet anodes were identical to trilayer pellets without the anode layer.

The Single Cell Discharge System

Single cells were discharged in the Platen Press Single Cell Tester Model 2 (Figure 2) which was based on the earlier design used in this laboratory (9) and the design by Bush (22,23).

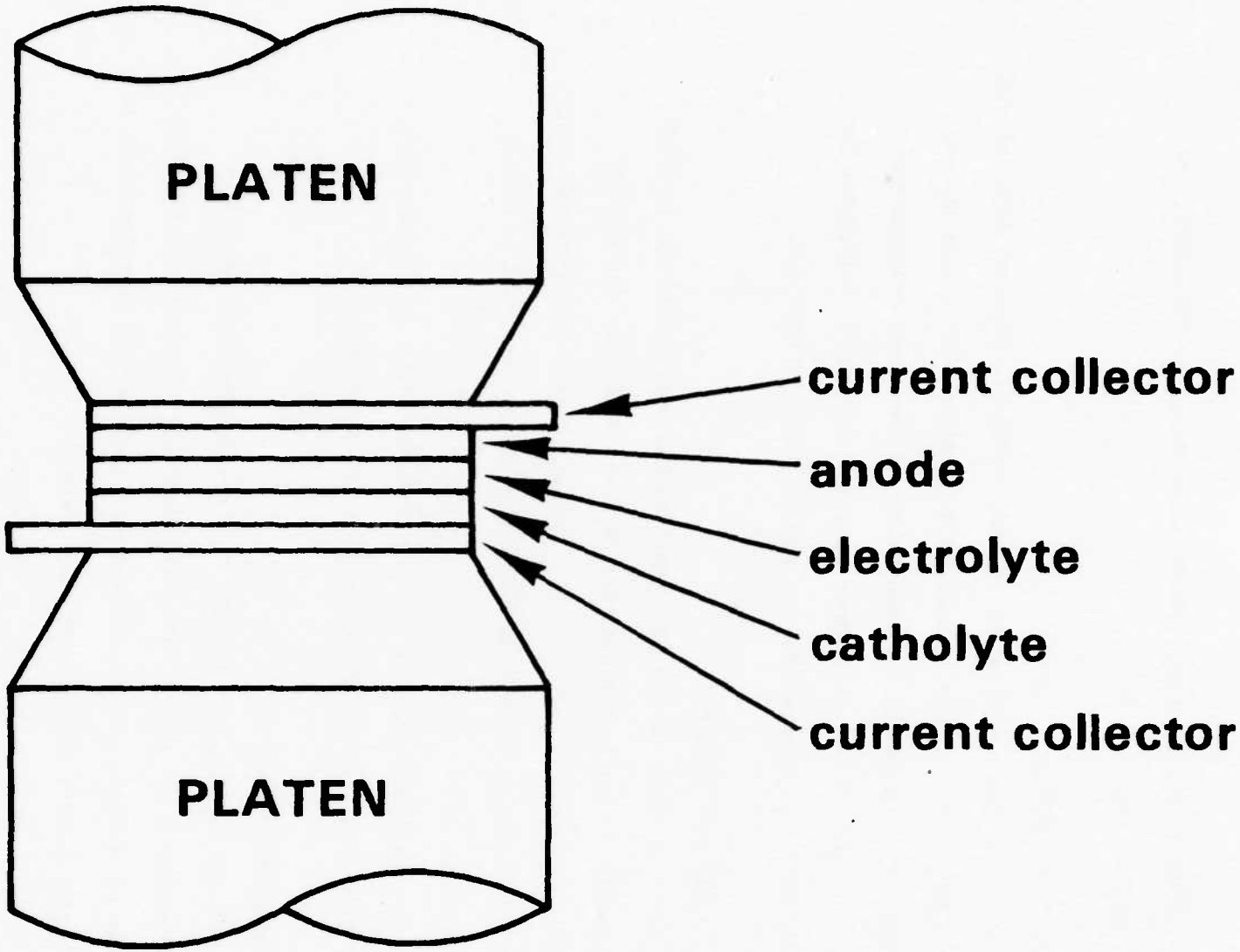

Figure 1: Typical Cell Configuration Between Heated Plates

Table I: Single Cell Pellet Composition and Compaction Pressures

Layer	Component	Weight[a,b] (g)	Pressure[c] (PSIA)
Anode	Al or Li-Al powder	0.500	16,700
	EB Mixture[d]	0.500	
Separator	EB Mixture[d]	0.900	23,000
Cathode	EB Mixture[d]	0.450	29,200
	$CuCl_2$	0.500	
	Graphite	0.160	

[a]All components were weighed to ±0.005 g.

[b]Total single cell weight was not allowed to vary more than ±2%.

[c]All pressures were regulated to ±400 PSIA.

[d]EB Mixture: Electrolyte (49.85 m/o AlCl-50.15 m/o NaCl) + 10 w/o Binding Agent (Cab-O-Sil).

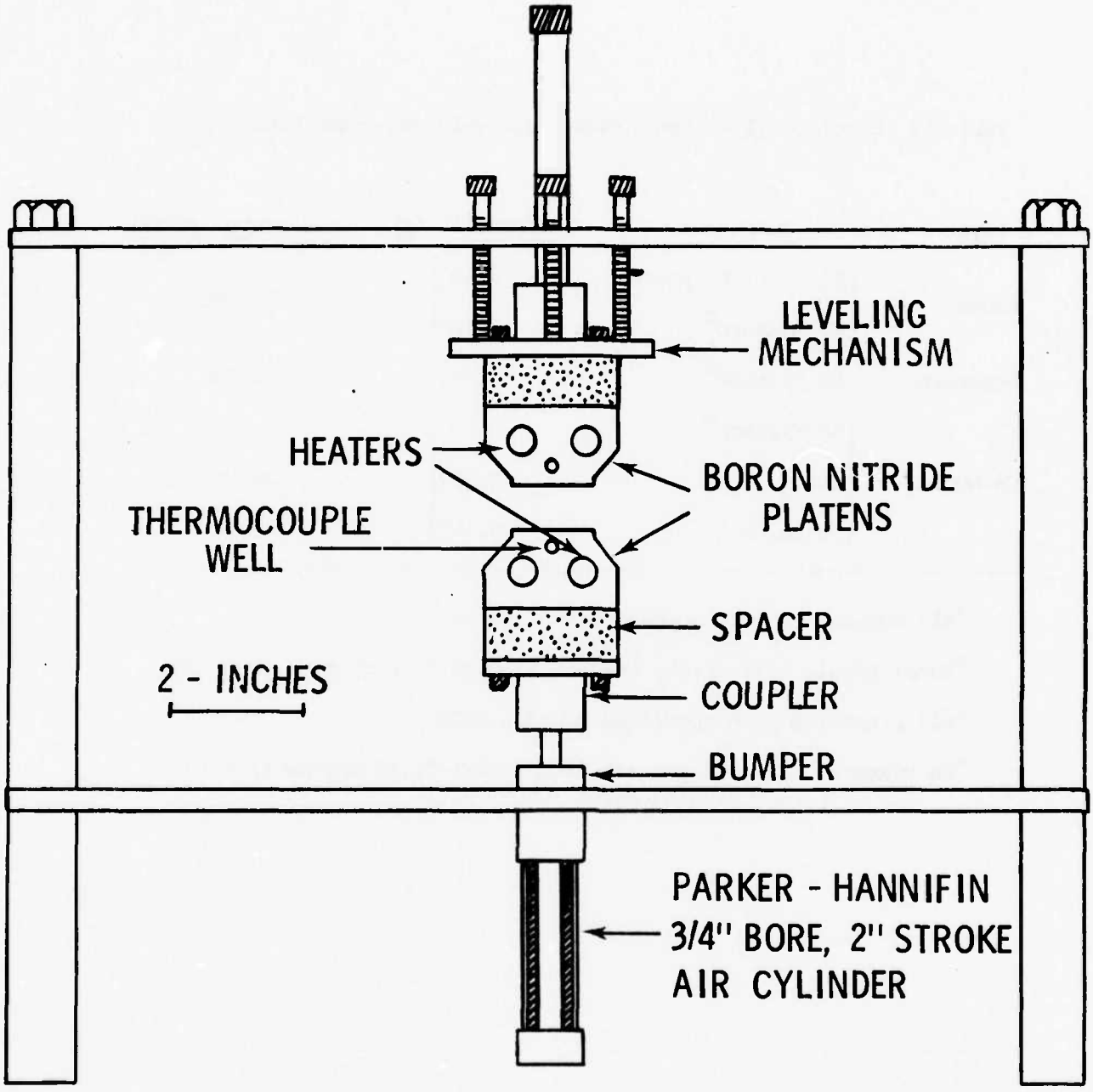

Figure 2: Platen Press Single Cell Tester - Model 2

The platen heads were heated by means of two Thunderbolt TB-381, 120V, 100 watt cartridge heaters (Vulcan Electric, Inc.) in each platen wired in parallel to an Electromax III Controller (Leeds and Northrup, Inc.). Chromel-alumel thermocouples were used as temperature sensors. Temperature readout was obtained from an ice/water referenced chromel-alumel thermocouple to a DANA Model 5330/700 digital multimeter (DMM). The analog output from the DMM was recorded graphically using an H-P 7100B recorder. Each platen could be heated from room temperature to a stable 175°C in three minutes and be controlled to ±0.3°C. Overall temperature control during a single cell discharge experiment was ±0.5°C.

Pressure on the single cells during test was maintained at 3 ± 0.25 PSIA using high purity argon. Selection of 3 PSIA as the pressure for the single cell tests was based on:

1. The analogous work of Bush (22,23) on Ca/LiCl-KCl/$CaCrO_4$ single cells at 515°C, and

2. The design of our single cell tester which allowed the pellet and current collectors to shift as the electrolyte became molten at pressures below 3 PSIA.

Constant current discharge experiments were conducted as described previously (12). An additional set of leads was connected across the single cell which allowed the cell voltage to be sampled by a DEC PDP 11/10C Data Acquisition System (DAS). Cell voltage, time, coulombs, experimental energy density, and the digital voltage-time curve for each cell were output by the DAS. A copy of the BASIC program and sample output are included as Appendices A and B.

RESULTS AND DISCUSSION

Error Analysis

Single cell test data are used as a semi-quantitative measure of the performance capability of current thermal battery systems. Manufacturing and operational requirements for multi-cell batteries make it impossible to translate current state-of-the-art single cell data into a quantitative measure of performance characteristics. However, because single cell test data is used in a semi-quantitative manner, it is necessary to include some analysis of the relative error associated with the test data. An error analysis was performed using the procedure of Strobel (24). The experimental energy density (EED) is calculated from

$$\text{EED (W-Hr/lb)} = \frac{(i,\text{amp})(\varepsilon,\text{volts})(t,\text{min})(453.6\ \text{g/lb})}{(\text{cell mass } w,\ \text{g})(60\ \text{min/hr})} \tag{3}$$

The relative error, σ_{EED}, is given by the expression

$$\frac{\sigma_{EED}}{EED} = \left(\frac{\sigma_i^2}{i^2} + \frac{\sigma_\varepsilon^2}{\varepsilon^2} + \frac{\sigma_t^2}{t^2} + \frac{\sigma_w^2}{w^2}\right)^{1/2} \tag{4}$$

In order to calculate σ_{EED} one must have an estimate of each of the relative errors for current, voltage, time, and the cell mass. These values are easily obtained from the manufacturer's equipment specifications and self imposed limits on each of the weights of components used to make each cell. For example, the relative error in the current is due to the ±0.001 volt stability of the PAR 371 Potentiostat/Galvanostat and the measured value of the constant current resistor, 4.914 ± 0.001 Ω. These values yield, for a constant current of 15.0 mA/cm^2, a σ_i^2/i^2

error equal to 4.399×10^{-6}. Similar calculations for $\sigma_\varepsilon^2/\varepsilon^2$ and σ_t^2/t^2 gave 5.96×10^{-8} and 1×10^{-10} respectively.

The major portion of the relative error in the experimental energy density is due to the errors in the cell mass, w. The relative error in w is given by

$$\frac{\sigma_w^2}{w^2} = \frac{(0.02w)^2}{(w)^2} + \frac{(0.005)^2}{(w_i)^2} \tag{5}$$

where w is the total weight of the pellet, and w_i is the individual weights of the single cell components. For an allowable error of 2% in the pellet weight and 0.005 g deviation in the weight of each individual component σ_w^2/w^2 is 1.83×10^{-3}. The sum of the terms in equation 4 is 0.0477. An additional factor in the overall experimental relative error is the platen press pressure which was 3 PSIA ± 5%. Whether the press pressure error adds directly to the experimental energy density error is unknown, but Bush (22,23) has shown that for pressures between 2 and 3 PSIA there is no adverse effect on activated life to 80% of peak voltage for Ca/LiCl-KCl/$CaCrO_4$ single cells between 475 and 550°C at 60 mA/cm^2.

Graphite Studies

The first set of experiments were concerned with the effects of using different manufacturers' graphite and the effect of graphite purity. Three commercial graphites and a purified one were evaluated. The results are summarized in Table II and Figure 3.

The unpurified Superior graphite gave the best results for energy density and total charge delivered, Run No. 1004-32. The purified Superior graphite gave a more uniform discharge curve with a slightly

Table II. Discharge Behavior as a Function of Different Graphites at 3.95 mA/cm^2 and 175°C[a]

Run No.	Manufacturer	OCV[b] (Volts)	iR Drop (Volts)	COV[d]: 0.8 Volts Lifetime (min)	Energy Density (W-Hrs/lb)	Charge (Coul)
1004-24	Alfa/Ventron	1.826	0.039	129	13.0	194
1004-28	Superior-Purified	1.831	0.039	118	12.2	177
1004-32	Superior-Unpurified	1.826	0.029	139	14.4	208
1004-36	Fisher	1.826	0.049	143	13.7	143

[a]Cell configuration identical to that given in Table I.

[b]OCV - Open Circuit Voltage

[c]COV - Cut Off Voltage

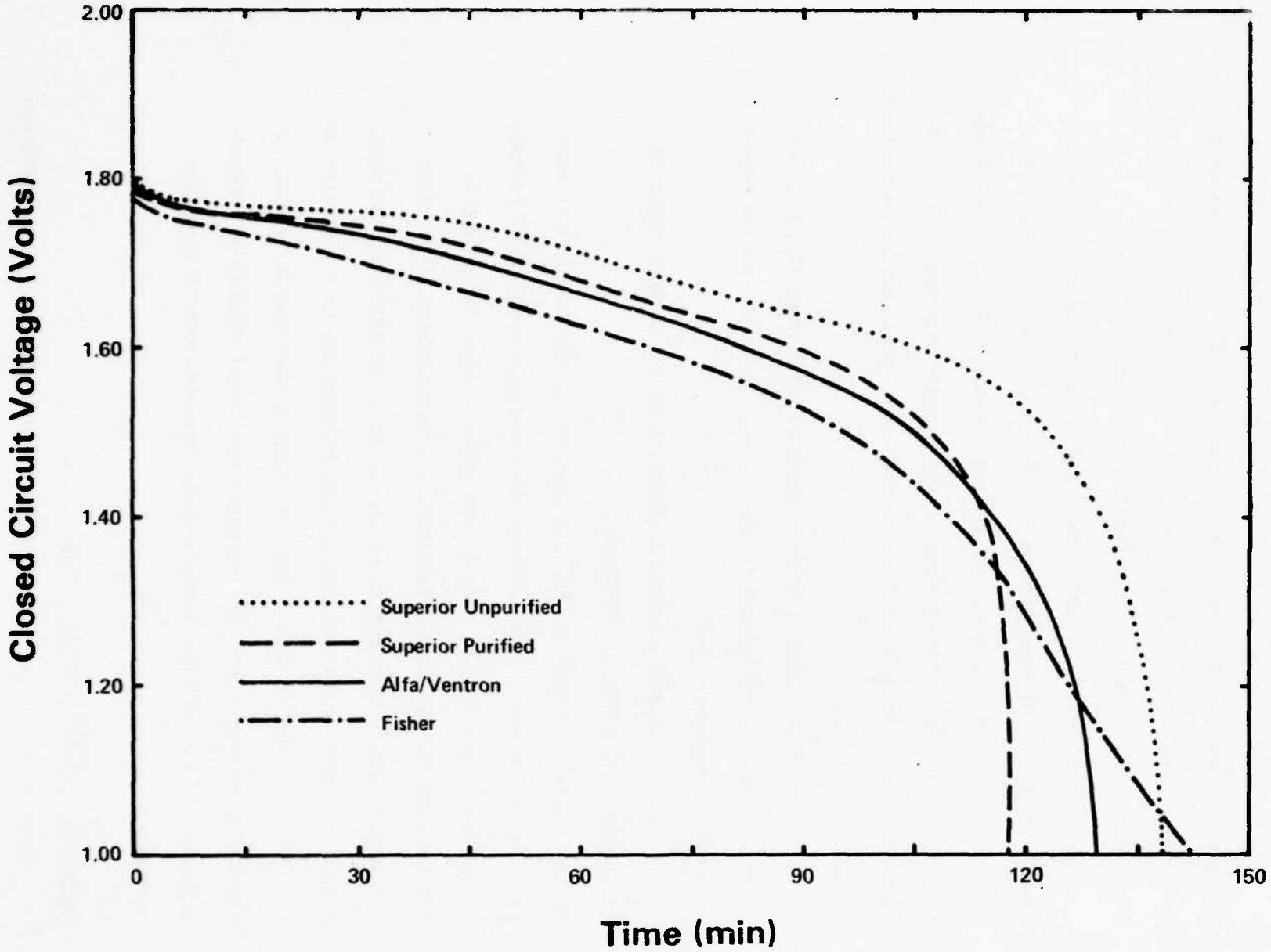

Figure 3: Discharge Behavior as a Function of Different Graphites at 3.95 mA/cm^2 and 175°C

flatter high voltage portion and a sharper drop off. This type of discharge curve was considered more desirable for reproducibility and all future experiments utilized the purified Superior graphite.

The second series of experiments utilizing graphite evaluated the dependence of the discharge curve on the quantity of graphite present in the cell. The results are summarized in Table III and Figure 4 and indicate a maximum in energy density and charge delivered at 0.21 g of graphite as well as a flatter discharge curve. This maximum is believed to be the result of:

a. Better contact between the $CuCl_2$ and graphite particles which improves the efficiency of the cathodic reaction, as the quantity of graphite increases, and

b. Decreased structural stability of the cathode layer as the quantity of graphite increases.

As the graphite content of the cathode layer in the pellet increases there is an increased difference in the expansion coefficient between the cathode layer and the rest of the pellet. When the pellet is removed from the die during fabrication this expansion coefficient difference causes delamination of the pellet. In addition, the more graphite present the weaker the cathode becomes due to a reduction in the percent binder in that layer; it crumbles more easily. These two physical problems offset the increased electrical contact and result in a peak in the cell performance under constant current discharge conditions.

Copper(II) Chloride Particle Size

Examination of the $CuCl_2$ cathode material showed a large variation

Table III: Discharge Behavior as a Function of Graphite Content at 15.0 mA/cm^2 and 200°C[a]

Run No.	Graphite Wt (g)	Total Cell Wt (g)	OCV[c] (Volts)	iR Drop (Volts)	COV[d]: 0.8 Volts Lifetime (min)	Energy Density (W-Hrs/lb)	Charge (Coul)
1006-40	0.110	2.950	1.831	0.122	60.7	13.1	350
1006-38	0.160	2.995	1.831	0.093	56.0	17.5	324
1006-34	0.210	3.060	1.831	0.083	59.0	19.4	341
1006-42	0.260	3.070	1.834	0.090	50.0	16.7	289

[a]Cell Configuration

Anode	0.500g LiAl (48 a/o) 0.500g EB Mixture[b]
Separator	0.900g EB Mixture[b]
Cathode	0.450g EB Mixture[b] 0.500g $CuCl_2$ (50-100 mesh) Graphite (Superior-purified), as indicated in the 2nd column

[b]EB Mixture: Electrolyte (49.85 m/o $AlCl_3$-50.15 m/o NaCl) + 10 w/o Binding Agent (Cab-O-Sil)

[c]OCV - Open Circuit Voltage

[d]COV - Cut Off Voltage

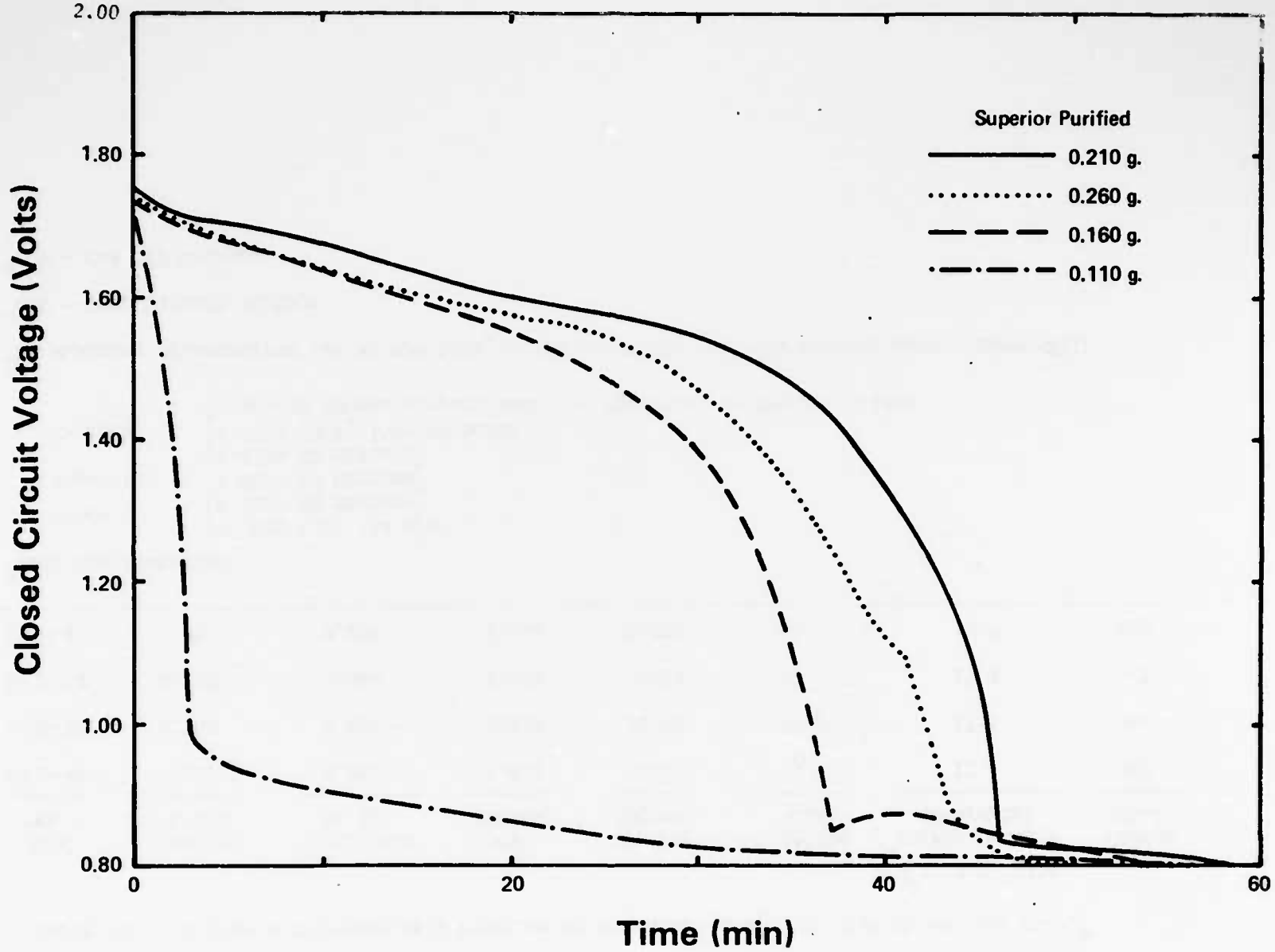

Figure 4: Discharge Behavior as a Function of Graphite Content at 15.0 mA/cm^2 and 200°C

in particle size. This variation was causing lack of reproducibility of single cell discharge data and occasional pellet fabrication problems. To eliminate these difficulties some of the $CuCl_2$ was ground in a CRC Micro-Mill and tested in a single cell. Performance of this cell was worse than for unground stock $CuCl_2$. The performance degradation could be due to an optimum particle size present in unground $CuCl_2$, or decomposition of the ground $CuCl_2$ while exposed to atmospheric moisture and oxygen during transfer between Dri-Boxes. To test the two possibilities, half the stock $CuCl_2$ was sieved and a fresh sample was ground under inert atmosphere conditions in the same Dri-Box that was used for the single cell tests. After the initial test data confirmed both possibilities, further tests were conducted on some of the sieved samples of $CuCl_2$ to elucidate particle size-current density and particle size-temperature effects. These latter tests were to define an optimum particle size for more extensive current density and temperature studies. The results of the $CuCl_2$ particle size studies are reported in Table IV.

Several conclusions may be drawn from the data in Table IV:

1. A comparison of runs 1005-18 and 1004-20 confirm degradation of the ground $CuCl_2$ by exposure to atmospheric moisture and oxygen.

2. At a low current density discharge, smaller $CuCl_2$ particles, >100 mesh, perform better than larger ones.

3. The 50-100 mesh particle size optimizes single cell performance over the current density and temperature ranges of interest. Subsequent studies on anodes, current density, and temperature utilized the 50-100 mesh $CuCl_2$.

Table IV: Discharge Behavior as a Function of $CuCl_2$ Particle Size[a]

Run No.	Temperature (°C)	Current Density (mA/cm^2)	Particle Size (ASTM Mesh)	OCV[c] (Volts)	iR Drop (Volts)	COV[d]: 1.0 Volts Lifetime (min)	Energy Density (W-Hrs/lb)	Charge (Coul)
1005-2	175	3.95	<30	1.826	0.037	86.0	8.98	129
1005-6	175	3.95	30-50	1.824	0.037	148.7	15.0	223
1005-10	175	3.95	50-100	1.824	0.037	201.3	19.2	302
1005-14	175	3.95	>100	1.821	0.032	203.0	19.9	304
1005-18	175	3.95	Ground	1.829	0.054	138.0	14.1	207
1004-20	175	3.95	Ground	1.831	0.058	55.0	5.26	82.5
1006-2	175	60.0	50-100	1.831	0.244	6.65	8.55	153.5
1006-6	175	60.0	30-50	1.826	0.232	2.55	3.44	58.8
1006-44	250	15.0	>100	1.875	0.549	1.5	0.48	10.6
1008-18	250	15.0	50-100	1.873	0.151	10.0	3.35	57.8

[a]Cell Configuration

Anode	0.500g LiAl (48 a/o) 0.500g EB Mixture[b]
Separator	0.900g EB Mixture[b]
Cathode	0.450g EB Mixture[b] 0.500g $CuCl_2$ (particle size - see 4th column) 0.160g Graphite (Superior-purified)

[b]EB Mixture: Electrolyte (49.85 m/o $AlCl_3$-50.15 m/o NaCl) + 10 w/o Binding Agent (Cab-O-Sil)

[c]OCV - Open Circuit Voltage

[d]COV - Cut Off Voltage

Aluminum, Lithium, and Lithium Aluminum Alloy Anodes

During the early part of this study Al, Li, and 48 a/o LiAl alloy were the available anodes for testing. From single cell test data, the 48 a/o alloy was selected as the anode to be used for current density and temperature studies. Other LiAl alloys became available later and were also tested. The 60.2 and 70.4 a/o alloys proved superior to the 48 a/o alloy, but to preclude lengthy retesting the current density and temperature studies were completed using the 48 a/o alloy. Discharge data for all the anodes tested were recorded to a cut off voltage, COV, of zero volts to determine overall coulombic and experimental energy density efficiencies. The results of the anode study are reported in Table V and Figures 5A and 5B.

Initial tests which coupled pure Al and the 48 a/o alloy with the $CuCl_2$ cathode indicated that the cell output was enhanced considerably using the alloy anode. The enhanced cell output could be due to:

1. Prevention of formation of an oxide coating on Al by alloying it with Li.

2. Removal of the oxide coating by reaction with the Li during cell discharge.

3. The actual cell discharge reaction being a mixed potential with both the Li and the Al coupled to the $CuCl_2$.

The test data also showed a high voltage spike during cell activation with the LiAl alloy which was not present with the pure Al anode (Figure 6A). The magnitude of the voltage spike suggested that it is due to participation of Li in the cell reaction (25,26). This supposition was verified using a pure Li anode (Figure 6C) which showed an identical spike.

Table V: Discharge Behavior as a Function of Different Anodes at 15.0 mA/cm^2 and 175°C[a]

Run No.	Anode	Anode[c] Wt (g)	Cell Wt (g)	OCV[d] (Volts)	iR Drop (Volts)	COV[e]: 0.0 Volts Lifetime (min)	Energy Density (W-Hr/lb)	Charge (Coul)
1006-26	Al powder	0.500	2.995	1.797	0.449	102.8	8.92	594
1008-12	Al plate	0.500	2.410	1.790	0.345	95.0	17.4	549
1008-24	48.0 a/0 LiAl powder	0.500	2.985	1.821	0.093	113.3	24.4	655
1008-22	60.2 a/o LiAl powder	0.500	2.995	1.831	0.110	116.0	27.8	670
1008-20	70.4 a/o LiAl powder	0.500	2.970	1.819	0.093	117.8	27.3	680
1008-4	90.9 a/o LiAl plate	0.630	2.610	1.926	0.188	104.0	21.7	601
1008-26	Li powder	0.078	2.068	1.909	0.225	34.0	11.9	196

[a]Cell Configuration

Anode	See table - Anode Material 0.500g EB Mixture[b]
Separator	0.900g EB Mixture[b]
Cathode	0.450g EB Mixture[b] 0.500g $CuCl_2$ (50-100) 0.160g Graphite (Superior-purified)

[b]EB Mixture: Electrolyte (49.85 m/o $AlCl_3$-50.15 m/o NaCl) + 10 w/o Binding Agent (Cab-O-Sil)

[c]No electrolyte - Cab-O-Sil mix was used in the anode in Run Nos. 1008-4,12, and 26

[d]OCV - Open Circuit Voltage

[e]COV - Cut Off Voltage

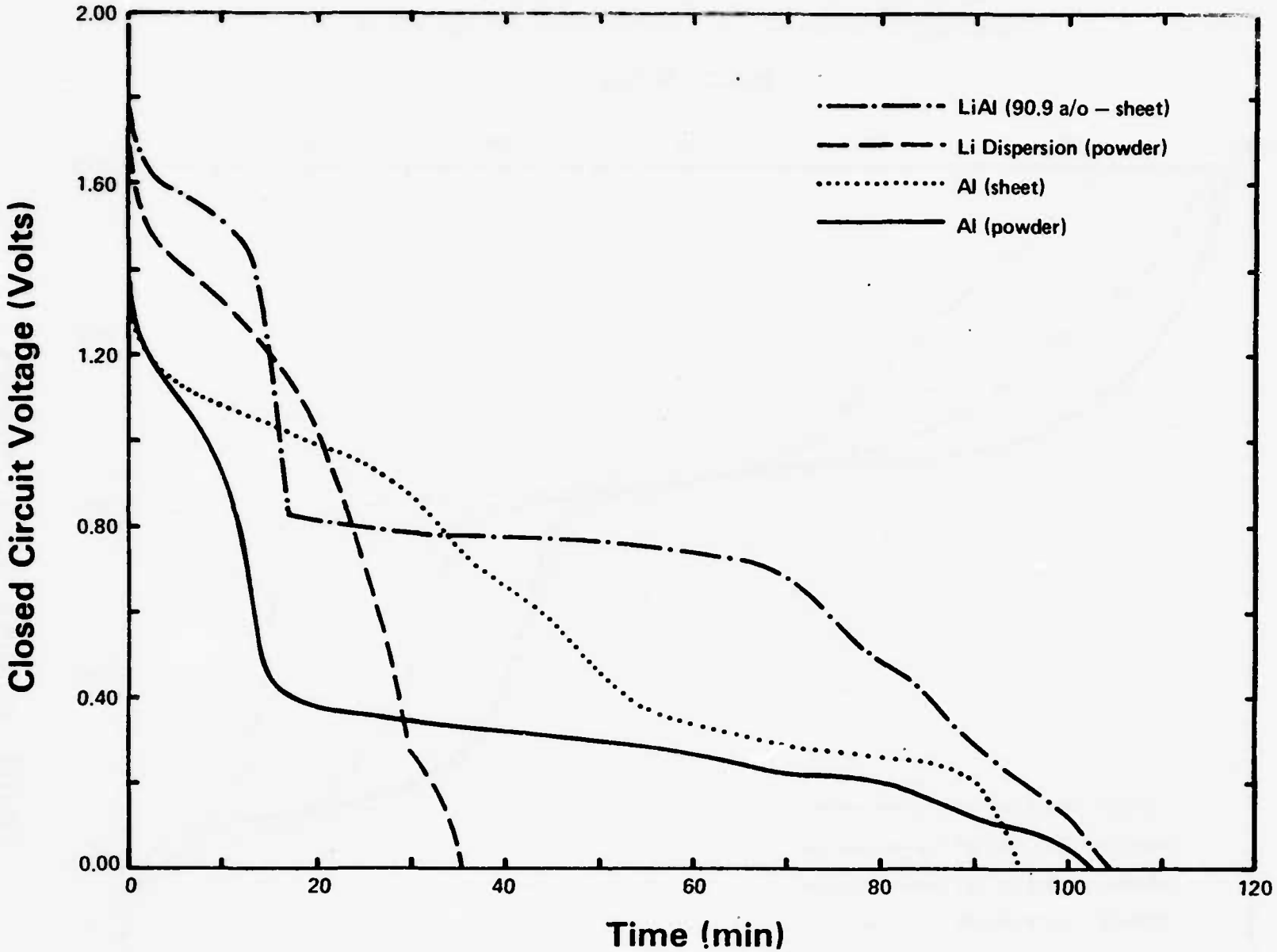

Figure 5A: Discharge Behavior as a Function of Different Anodes at 15.0 mA/cm^2 and 175°C for Li Dispersion, 90.9 a/o LiAl Alloy, Al Sheet, and Al Powder

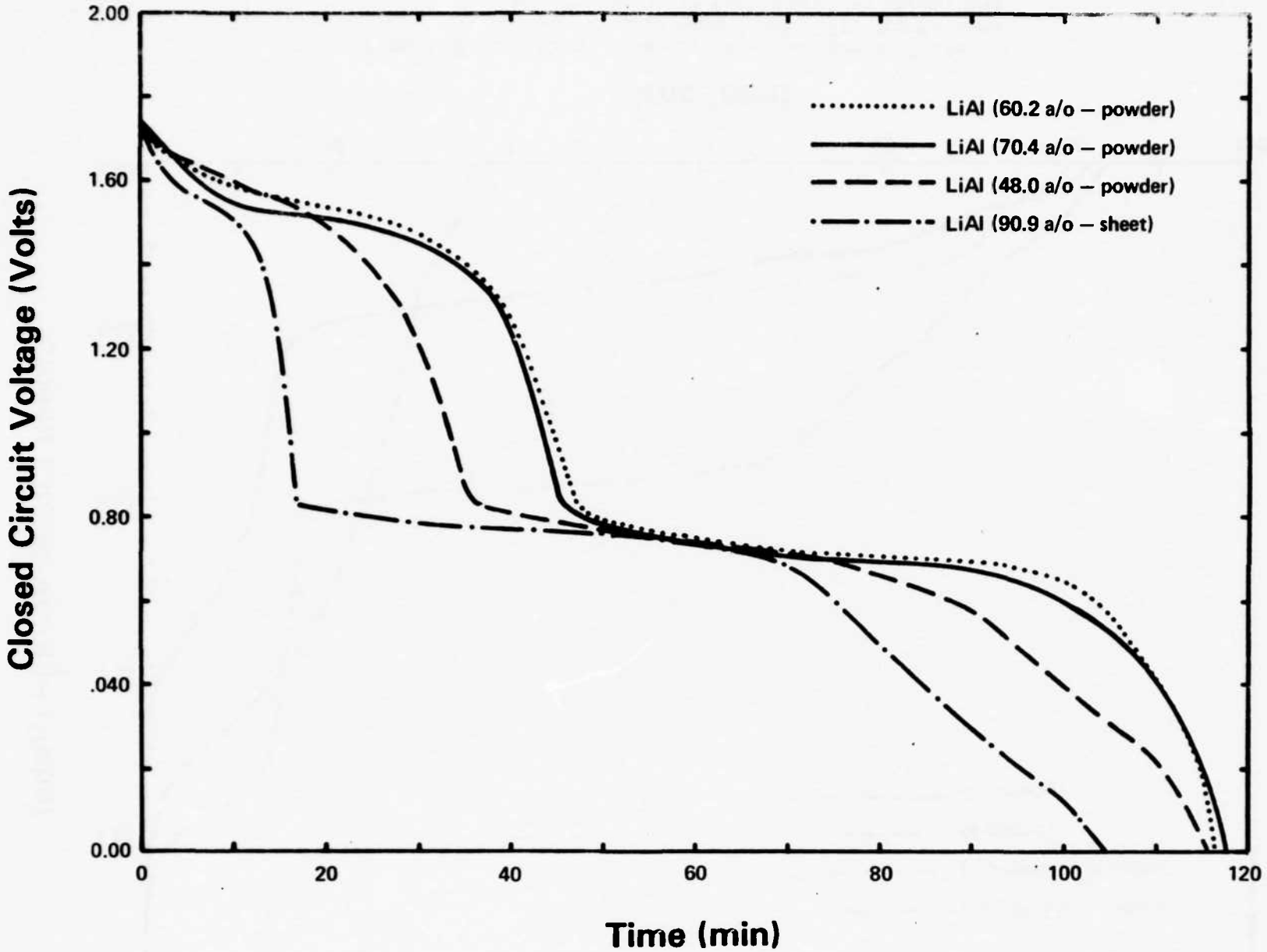

Figure 5B: Discharge Behavior as a Function of Different Anodes at 15.0 mA/cm^2 and 175°C for 90.9, 70.4, 60.2, and 48.0 a/o LiAl Alloys

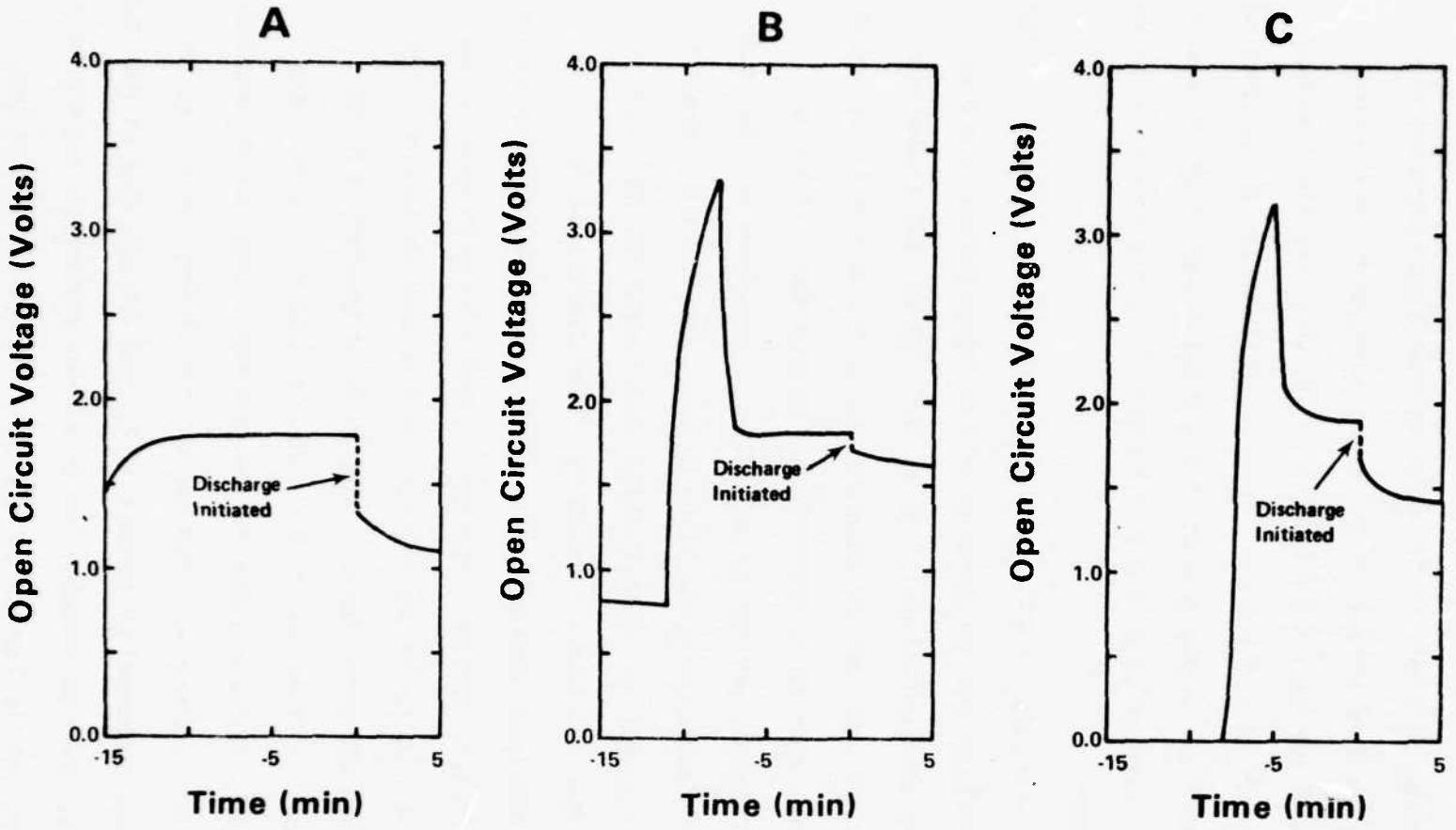

Figure 6: Voltage-Time Curves During Temperature Activation for (A) $Al/NaAlCl_4/CuCl_2$ Single Cell, (B) LiAl (48.0 a/o)/$NaAlCl_4/CuCl_2$ Single Cell, and (C) $Li/NaAlCl_4/CuCl_2$ Single Cell

The precipitous dropoff in the spike voltage always occurred at 155-160°C, the observed melting point of the electrolyte in a pellet. The OCV for the alloy then stabilized at 1.82V, very near the potential for the $Al/CuCl_2$ couple (Table V). These observations on the behavior of the Li and LiAl alloy anodes suggest that a displacement reaction between the anode and the electrolyte occurs (reaction 6) at the melting point on the anode surface.

$$3\ Li + NaAlCl_4 \longrightarrow 3\ LiCl + NaCl + Al \qquad (6)$$

Further insight into the behavior of LiAl alloy anodes in a $NaAlCl_4$ electrolyte was obtained by analyzing the data for all the anodes tested. The experimental energy density increased as the content of Li increased in the alloy to a maximum at the 60-70 a/o composition. If the increased energy density was due to prevention of formation of the oxide coating on the aluminum when the alloy is made, then one would predict that the same increase in energy density should occur for any alloy regardless of the Li content. Similarly if the function of the Li is to react with the oxide coating on the Al then the discharge data should show no trend with Li content. The data in Table V and Figures 5A and 5B clearly show this is not the case and tend to substantiate the third supposition that the anode discharges as an Al or possibly a mixed potential anode. Differences in the discharge data for the 90.9 a/o alloy and pure Li anodes compared to the powdered alloys can be attributed to increased cell resistance. From Table V the iR drop under load for these two anodes increased by factors of 1.7 and 2.0 relative to the 60.2 a/o LiAl anode. This is probably due to contact resistance for the 90.9 a/o alloy sheet and the lack of an electrolyte-Cab-O-Sil mix in the anode section of the pellet for the powdered Li. Unfortunately, the

90.9 a/o alloy was not available in powdered form and the Li powder could not be pelletized even with 20 times the usual amount of EB mix added to it.

Comparison of the discharge data for the three powdered alloy anodes would be extremely difficult except that the 60.2 and 70.4 a/o alloys gave essentially identical results, the 48 a/o alloy experimental energy density data fell outside the 4.77% relative error discussed earlier, and the voltage-time trace for the 48 a/o alloy is markedly different from the other two powdered alloys (Figure 5B). The results indicate that the 48.0 a/o alloy discharge mechanism may be different from the others. Examination of the LiAl phase diagram (27) and the study by James (25,26) of the LiAl anode in the LiCl-KCl eutectic electrolyte suggest the differences are probably due to the presence of the γ-phase alloy, the compound Li_2Al. James presents evidence that the γ-phase alloy is difficult to form on charging and that the β-phase, the compound LiAl, is not. These observations suggest the equilibrium constants for the dissociation of Li_2Al and the formation of LiAl are large.

Recent work by Myles et al. (28) has further delineated the LiAl phase diagram. They established the limit for β-LiAl at 48 a/o and found the γ-phase was Li_3Al_2, not the previously reported Li_2Al (26). They were also able to identify a δ-phase compound, Li_9Al_4. Based on the work of James and the modification reported by Myles et al., it is suggested that dissociation of the γ and δ-phases to produce free Li occurs more easily that dissociation of the β-phase. Assuming the β-phase has a higher stability than the 70.4 (δ) and the 60.2 (γ) a/o alloys, the latter two can more easily supply the Li necessary to sustain the discharge reaction than the 48 (β) a/o alloy.

The actual electrochemical reaction which takes place during the cell discharge is still not clear. Either reaction of the Al produced by Li reacting with the electrolyte, or direct reaction of Li produced by dissociation of the alloy anode could be the sustaining electrochemical reaction. The magnitude of the cell OCV at the discharge temperature as well as the behavior of the cell voltage during activation lend credence to the Li-electrolyte reaction.

Other data which must be considered prior to establishing a mechanism for the reaction of LiAl alloy anodes in a $NaAlCl_4$ electrolyte is the behavior of the 60.2 a/o alloy in the $LiAl/NaAlCl_4/MoCl_5$ thermal battery by Ryan and Bricker (29). They observed the temperature of the thermal battery under constant load discharge conditions to fall to 135°C during the active lifetime of the battery. The melting point of the electrolyte in a thermal cell observed in this laboratory during temperature activation is 155-160°C. These two pieces of data would seem to indicate either that the electrolyte is supercooling substantially, or the initial saturated binary electrolyte becomes unsaturated or a ternary electrolyte is formed as the battery and the cell discharge. If a Li-electrolyte reaction occurs (reaction 6, page 26), a ternary electrolyte containing LiCl is quite conceivable. However, there are several low melting $NaCl-AlCl_3$ electrolytes which are reported to contain as little as 4 m/o $MoCl_5$ (30), and the data reported by Nardi et al. (31) confirms that $MoCl_5$ does dissolve appreciably in the electrolyte. It is likely therefore that any one or a combination of these explanations are contributing factors in the observed low temperature of an operational thermal battery. Confirmation will depend on an analysis of the

single cell electrolyte after discharge and by mapping of the LiCl-NaCl-$AlCl_3$ phase diagram.

Based on the experimental data reported here, we propose a probable mechanism for the reaction of LiAl alloy anodes in NaCl saturated $AlCl_3$-NaCl electrolytes to be:

$$LiAl(\beta,\gamma, \text{ or } \delta) \xrightleftharpoons{K_D} LiAl(\alpha+\beta,\beta, \text{ or } \gamma+\delta) + Li$$

followed by

$$3\ Li + NaAlCl_4 \longrightarrow 3\ LiCl + NaCl + Al$$

$$Al + 4\ NaCl \rightleftharpoons NaAlCl_4 + 3\ Na^+ + 3e^-$$

and/or

$$Li + NaCl \rightleftharpoons LiCl + Na^+ + e^-$$

For a cathodic $2e^-$ reduction of $CuCl_2$,

$$CuCl_2 + 2\ Na^+ + 2e^- \rightleftharpoons Cu + 2\ NaCl$$

the overall reaction stoichiometry for the single cell is

$$LiAl(\beta,\alpha, \text{ or } \delta) + CuCl_2 \longrightarrow LiAl(\alpha+\beta,\beta, \text{ or } \alpha + \delta) + LiCl + Cu$$

Current Density

The performance of the LiAl/$CuCl_2$ couple to 80% of the Initial Closed Circuit Voltage (ICCV) was evaluated at current densities from 2.00 to 120 mA/cm^2. The 80% criteria was based on required performance specifications for numerous production thermal batteries. The results are reported in Table VI and Figure 7 and indicate the EED decreases as the current density increases. Similar behavior at 175°C has been observed in this laboratory utilizing a $MoCl_5$ cathode (31).

In evaluating the performance of an electrochemical couple, a determination of the cell resistance is necessary to determine the inherent current limitation of the cell. High values of cell resistance

Table VI: Discharge Behavior as a Function of Current Density at 175°C[a]

Run No.	Current (mA)	Current Density[c] (mA/cm^2)	ICCV[d] (Volts)	COV[e] (Volts)	Lifetime (min)	Energy Density (W-Hr/lb)
1006-22	12.8	2.00	1.824	1.459	301	16.7
1005-11	50.3	7.85	1.763	1.410	60.0	12.5
1006-14	96.3	15.0	1.738	1.383	30.4	11.8
1006-18	192	30.0	1.689	1.352	12.0	8.79
1006-2	385	60.0	1.587	1.270	4.37	5.94
1006-46	513	80.0	1.384	1.107	2.07	3.23
1008-6	641	100	1.315	1.052	1.08	1.96
1006-20	770	120	1.306	1.045	1.045	1.31

[a]Cell Configuration

Anode	0.500g LiAl (48 a/o) 0.500g EB Mixture[b]
Separator	0.900g EB Mixture[b]
Cathode	0.450g EB Mixture[b] 0.500g $CuCl_2$ (50-100 mesh) 0.160g Graphite (Superior-purified)

[b]EB Mixture: Electrolyte (49.85 m/o $AlCl_3$-50.15 m/o NaCl) + 10 w/o Binding Agent (Cab-O-Sil)

[c]Surface area of each cell was 6.41 cm^2

[d]ICCV - Closed Circuit Voltage at time zero

[e]COV - Cut Off Voltage measured to 80% of the ICCV

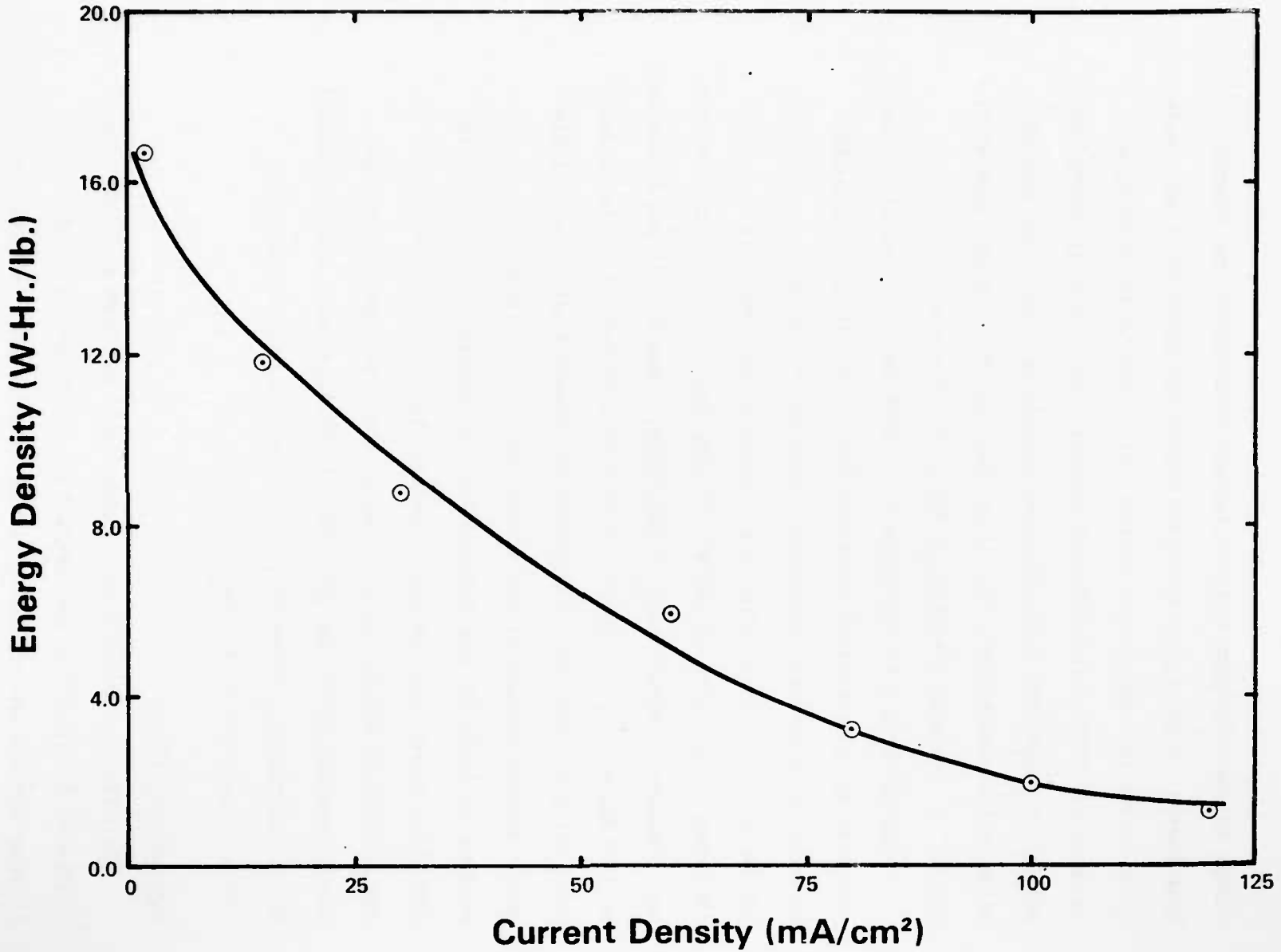

Figure 7: Energy Density to 80% of the ICCV as a Function of Discharge Rate at 175°C

result in low efficiency and poor battery performance from internal heat losses. A convenient and quick method for determining cell resistance is the two-step current method (32). This method requires a value of the ICCV at two different currents and is readily adapted to multiple measurements using graphical techniques. The least squares value of the resistance of the cells used over the current range studied was 0.72 Ω; the data are given in Table VI and Figure 8.

Variations in cell resistance as a function of the extent of discharge is an indication of the solubility of the discharge products. An increase in internal resistance indicates the products are generally not soluble; correspondingly, a decreasing or constant cell resistance indicates the products are soluble to some degree. To determine single cell resistance versus extent of discharge, a single cell was discharged at 15.0 mA/cm^2 for 10 minutes, followed by interruption of the current for 3 minutes. This cyclic discharge was repeated until the cell discharge voltage dropped to zero volts. The cell resistance values are reported in Table VII and indicate that the discharge products of the $CuCl_2$/LiAl couple are insoluble. As the discharge reaction changes to the Cu(I)/Cu(O) couple, the cell resistance drops again and remains fairly constant during the remainder of the discharge. This indicates the nonconducting passivating layer of CuCl is being replaced by electrically conducting elemental copper.

Temperature Effects

The effect of temperature on single cell performance is manifested by changes in the OCV as the temperature varies and by changes in the lifetime and the energy density output as cells are discharged at

Table VII: Cell Resistance as a Function of Extent of Discharge at 96.3 mA and 175°C

Cycle[c] No.	OCV[d] (Volts)	CCV[e] (Volts)	Resistance[f] (Ω)	Discharge[g] Fraction
1	1.816	1.733	0.86	0.000
2	1.812	1.702	1.14	0.085
3	1.741	1.624	1.22	0.170
4	1.699	1.545	1.60	0.254
5	1.685	1.443	2.51	0.339
6	1.653	1.179	4.92	0.424
7	1.018	0.813	2.13	0.508
8	0.918	0.686	1.37	0.593
9	0.894	0.762	1.37	0.678
10	0.884	0.740	1.50	0.763
11	0.878	0.720	1.62	0.848
12	0.872	0.703	1.76	0.932

[a]Cell Configuration

Anode	0.500g LiAl (48 a/o) 0.500g EB Mixture[b]
Separator	0.500g EB Mixture[b]
Cathode	0.500g EB Mixture[b] 0.500g $CuCl_2$ (50-100 mesh) 0.160g Graphite (Superior-purified)

[b]EB Mixture: Electrolyte (49.85 m/o $AlCl_3$-50.15 m/o NaCl) + 10 w/o Binding Agent (Cab-O-Sil)

[c]Cycle - 10 min discharge followed by 3 min recovery

[d]OCV - Open Circuit Voltage

[e]CCV - Closed Circuit Voltage at time zero for each cycle

[f]Resistance = (OCV - CCV)/0.0963 A

[g]Discharge Fraction = $\sum_{i=1}^{n}$ Coulombs / Total Coulombs where n is the cycle No.

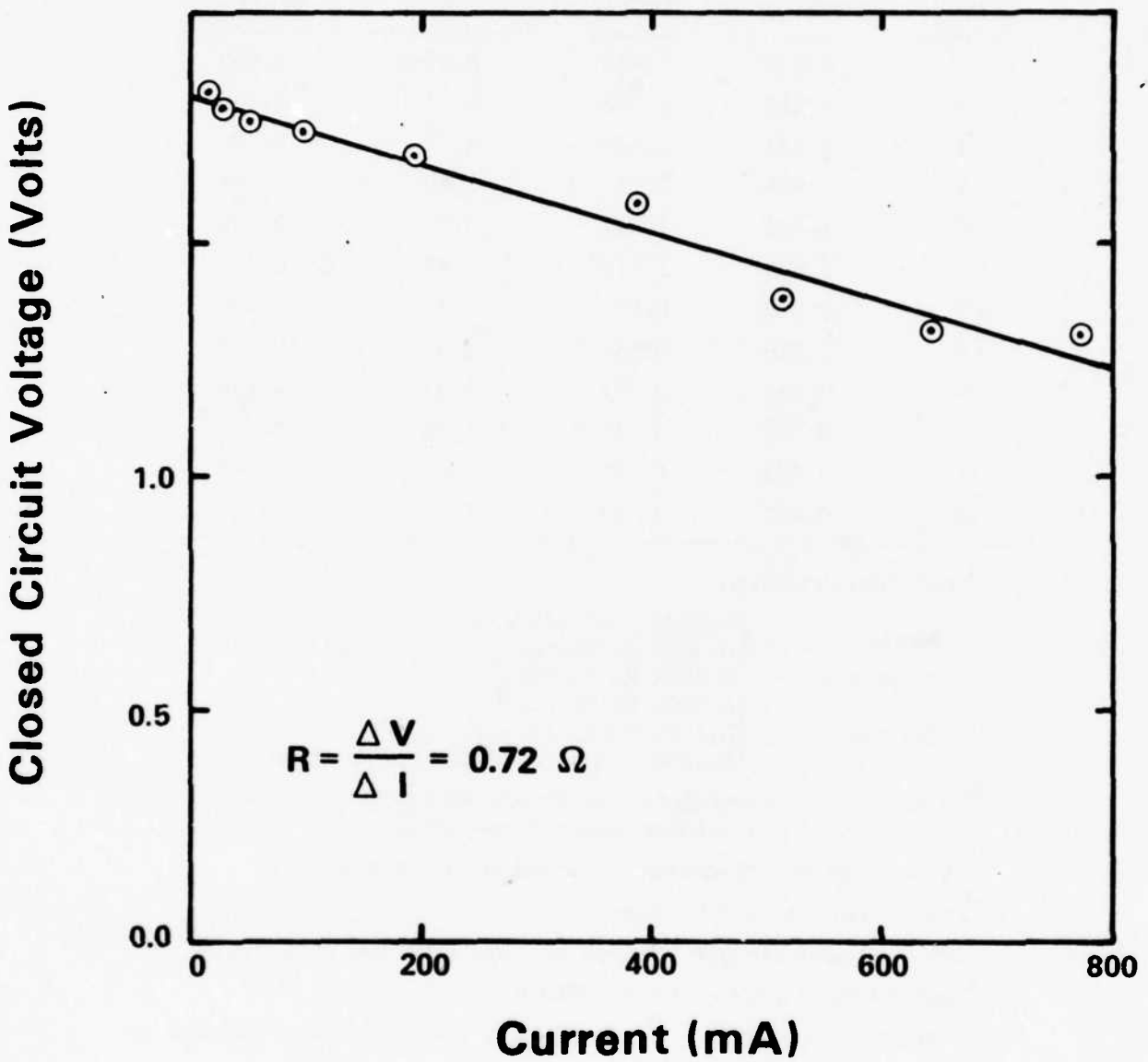

Figure 8: Closed Circuit Voltage as a Function of Current for a LiAl (48.0 a/o)/$NaAlCl_4$/$CuCl_2$ Single Cell at 175°C

different temperatures. The temperature dependence of the OCV was determined between 175 and 275°C and the data are reported in Table VIII and Figure 9. The figure clearly indicates that the temperature dependence of the OCV is nonlinear. The Nernst equation predicts a linear increase in the Cu(II)/Cu(I) half cell potential as temperature increases at a constant concentration of reactants and products. Boxall et al. (20) has indicated that Cu(II) is soluble in a chloride ion rich $AlCl_3$ electrolyte. The observed nonlinear increase in the OCV for the $CuCl_2$ cathode suggest that the solubility of $CuCl_2$ increases as the temperature increases, substantiating the results obtained by Boxall et al.

The effect of temperature on single cell discharge behavior was also studied. The results both to 80% of the ICCV and to zero volts are reported in Table IX. The overall cell lifetime did not vary appreciably as the temperature increased but the energy density output did. This was due to the shorter lifetime of the high voltage portion of the discharge curve. The data show an abrupt drop in the energy density to 80% of the ICCV at temperatures above 200°C, contrasted to a more gradual decrease in the energy density to zero volts. This difference is demonstrated graphically in Figure 10, and indicates the Cu(II)/Cu(I) couple is more dependent on temperature than the Cu(I)/Cu(0) couple.

The effect of temperature on cell voltage during cell activation furnished some useful data that correlated qualitatively with the discharge characteristics of single cells. Superior discharge performance was obtained after temperature stabilization when there was:

1. An observed cell voltage at room temperature of an undischarged cell.

Table VIII: Open Circuit Voltage as a Function of Temperature[a]

Temperature (°C)	OCV[c] (Volts)	S.D.[d] (Volts)	Number of Determinations
175	1.825	±0.004	20
200	1.832	±0.004	6
225	1.845	?	1
250	1.874[e]	±0.001	2
275	1.907	?	1

[a]Cell Configuration

Anode	0.500g LiAl (48.0 a/o) 0.500g EB Mixture[b]
Separator	0.900g EB Mixture[b]
Cathode	0.450g EB Mixture[b] 0.500g $CuCl_2$ (50-100 mesh) 0.160g Graphite (Superior-purified)

[b]EB Mixture: Electrolyte (49.85 m/o $AlCl_3$-50.15 m/o NaCl) + 10 w/o Binding Agent (Cab-O-Sil)

[c]OCV - Open Circuit Voltage

[d]S.D. - Standard Deviation

[e]One of the two cells utilized $CuCl_2$ (>100 mesh)

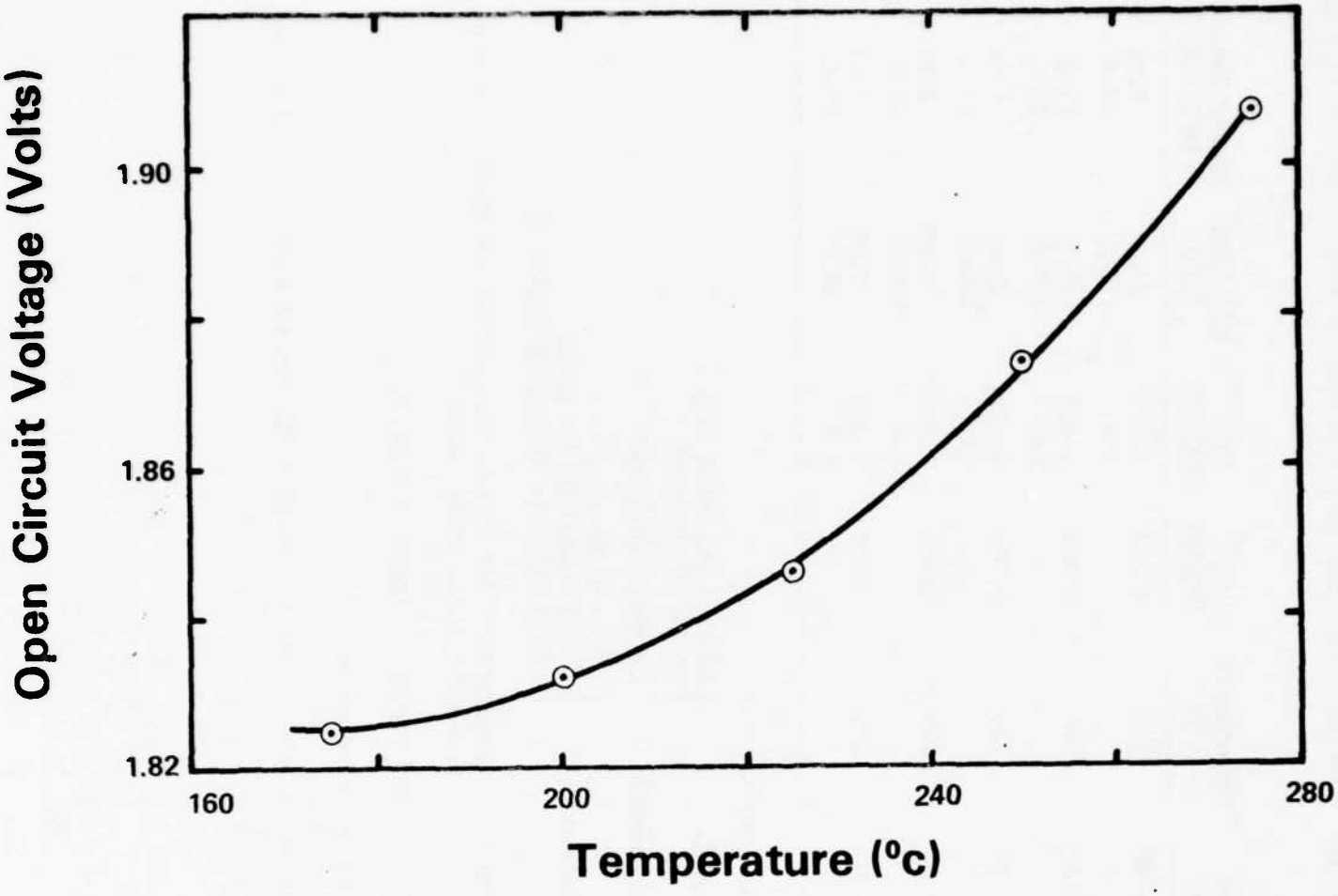

Figure 9: Open Circuit Voltage of a LiAl (48.0 a/o)/ $NaAlCl_4/CuCl_2$ Single Cell as a Function of Temperature

Table IX: Discharge Behavior as a Function of Temperature at 15.0 mA/cm^2[a]

Run No.	Temperature (°C)	ICCV[c] (Volts)	COV[d,e] (Volts)	Lifetime[e] (min)	Energy Density[e] (W-Hr/lb)
1006-48	175	1.733	1.387	23.5	8.99
			0.0	112.2	23.6
1006-38	200	1.738	1.391	29.7	11.5
			0.0	110.6	26.6
1006-36	225	1.768	1.414	21.0	5.58
			0.0	119.5	27.9
1008-18	250	1.721	1.377	5.63	2.18
			0.0	110.3	22.1
1008-10	275	1.812	1.450	7.25	2.97
			0.0	92.0	19.4

[a]Cell Configuration

Anode	0.500g LiAl (48.0 a/o) 0.500g EB Mixture[b]
Separator	0.900g EB Mixture[b]
Cathode	0.450g EB Mixture[b] 0.500g $CuCl_2$ (50-100 mesh) 0.160g Graphite (Superior-purified)

[b]EB Mixture: Electrolyte (49.85 m/o $AlCl_3$-50.15 m/o NaCl) + 10 w/o Binding Agent (Cab-O-Sil)

[c]ICCV - Closed Circuit Voltage at time zero

[d]COV - Cut Off Voltage

[e]First entry of each set to 80% of ICCV; second entry to zero volts.

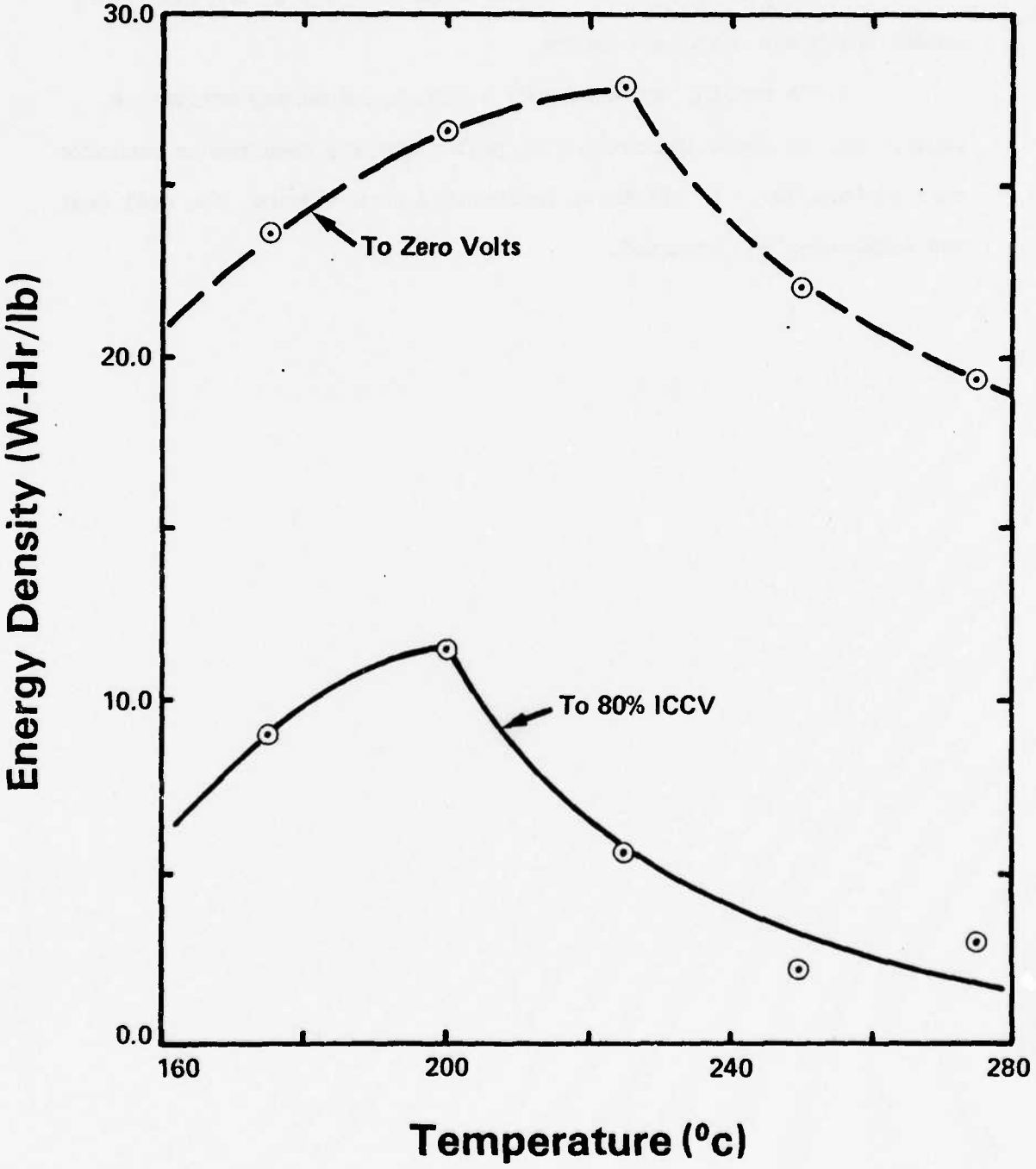

Figure 10: Energy Densities as a Function of Temperature

2. A peak in the OCV - time trace for pure Li and LiAl alloy anodes which was sharp and narrow.

3. A smooth, non-noisy OCV - time trace during activation. Lack of any of these indications of pellet quality resulted in mediocre cell performance. If all three indications were missing, the cell test was terminated and repeated.

CONCLUSIONS

Single cell studies of the $LiAl/NaAlCl_4/CuCl_2$ electrochemical system have shown that it is an excellent candidate for a long life thermal battery. Energy density to 80% of the ICCV at 15.0 mA/cm^2 at 200°C was 11.5 W-Hr/lb in a cell with a 48.0 a/o LiAl alloy anode. Significant improvement was obtained using the 60.2 a/o LiAl alloy anode. The effect of the various parameters studied on single cell performance was to:

1. Vary the energy density output by 20%, depending on the type of graphite used and the pretreatment received by the graphite.

2. Increase the energy density output to 80% of the ICCV by increasing the graphite content of the cathode from 0.16 g to an optimum 0.21 g (at 15.0 mA/cm^2 and 200°C).

3. Vary the energy density output with the particle size of the $CuCl_2$. Optimum energy density output from 175 to 275°C and from 3.95 to 60 mA/cm^2 was obtained using 50-100 ASTM mesh size $CuCl_2$.

4. Increase the energy density to 80% ICCV by increasing the Li content of the alloy anode from 48.0 to 60.2 a/o. Coulombic efficiency was 96.5% at 15.0 mA/cm^2 at 175°C utilizing the 60.2 a/o LiAl alloy.

5. Determine the average cell resistance, 0.72 Ω, over the current range 2 to 120 mA/cm^2.

6. Increase the cell resistance as a function of the discharge fraction to a maximum 4.92 Ω at 42.4% of total discharge followed by a drop in resistance for the remainder of the discharge. This behavior was attributed to decreased solubility of the discharge products for

the Cu(II)/Cu(I) couple, and to increased electrical conductivity of the discharge products of the Cu(I)/Cu(O) couple.

7. Observe a nonlinear relationship between the OCV and temperature which was attributed to increased solubility of the $CuCl_2$ in the electrolyte at higher temperatures.

8. Have a maximum experimental energy density in the 200 to 225°C temperature region.

Future studies of the Al alloy/$NaAlCl_4$/$CuCl_2$ electrochemical system should include:

1. Optimization of electrolyte/active ingredient ratios.

2. Performance characterization of aluminum anodes containing alloyed metals which are electrochemically less active than lithium. This should be aimed at eliminating the voltage spike observed prior to discharge with Li and LiAl alloy anodes.

3. A determination of the thermodynamic properties for LiAl alloys to enable estimates of theoretical energy densities to be made.

4. Mapping of the LiCl-NaCl-$AlCl_3$ phase diagram which is probably the actual electrolyte in the LiAl/$NaAlCl_4$/$CuCl_2$ pelletized thermal cell.

REFERENCES

1. B.H. Van Domelen and R.D. Wehrle, "A Review of Thermal Battery Technology," Proceedings 9th Intersociety Energy Conversion Engineering Conference, ASME, 1974.
2. C.W. Jennings, "Thermal Batteries," The Primary Battery, Vol. Two, N.C. Cahoon and G.W. Hesse, Ed., John Wiley and Sons, Inc., New York, 1976, pp 263-293.
3. R.D. Wehrle and B.H. Domelen, "Long-Life Thermal Battery Studies," Report SLA-73-0459, Sandia Laboratories, Albuquerque, NM, June 1973.
4. A.R. Baldwin, "A Long-Life Low Voltage, Power Thermal Battery," Proceedings 26th Power Sources Symposium, PSC Publications Committee, Red Bank, NJ, 1974, pp 137-141.
5. D.M. Bush and A.R. Baldwin, "A Preliminary Study into the Feasibility of a Sixty-Minute Thermal Battery," Report SLA-73-0412A, Sandia Laboratories, Albuquerque, NM, reprinted July 1974.
6. D.M. Bush, "A Sixty Minute Thermal Battery," Report SAND-75-0454, Sandia Laboratories, Albuquerque, NM, March 1976.
7. A. Baldwin, "A Sixty Minute Thermal Battery," Proceedings 27th Power Sources Symposium, PSC Publications Committee, Red Bank, NJ, 1976, pp 152-154.
8. W.S. Bishop and A.A. Benderley, "Critical Materials in Thermal Batteries," ibid., pp 158-160.
9. G.D. Brabson, J.K. Erbacher, L.A. King and D.W. Seegmiller, "Exploratory Aluminum-Chlorine Thermally Activated Battery: Single Cell Experiments," Report SRL-TR-76-0002, F.J. Seiler Research Laboratory (AFSC), USAF Academy, CO, January 1976.

10. B.W. Mulligan, "Low Temperature Thermal Batteries," Proceedings 27th Power Sources Symposium, PSC Publications Committee, Red Bank, NJ, 1976, pp 147-151.

11. F.C. Krieger, "Fusible Heat Reservoirs for Thermal Batteries," Proceedings 26th Power Sources Symposium, PSC Publication Committee, Red Bank, NJ, 1974, pp 129-133.

12. C.L. Hussey, J.K. Erbacher and L.A. King, "High Energy Density Pelletized Aluminum Chloride Thermal Batteries," Report SRL-TR-76-0003, F.J. Seiler Research Laboratory (AFSC), USAF Academy, CO, January 1976.

13. R. Jasinski, J. Electroanal. Chem., 26, 189 (1970).

14. M. Eisenberg, R.E. Kuppinger and K.M. Wong, J. Electrochem. Soc., 117, 557 (1970).

15. M. Eisenberg and K. Wong, J. Hydronautics, 5, 97 (1971).

16. G. Eichinger and J.O. Besenhard, J. Electroanal. Chem., 72, 1 (1976).

17. M. Eisenberg, "The Cupric Chloride-Lithium Organic Electrolyte Primary Battery for Very High Rate Applications," Proceedings 27th Power Sources Symposium, PSC Publications Committee, Red Bank, NJ, 1976, pp 56-59.

18. S.C. Levy and F.W. Reinhardt, "Thermal Battery Cathode Studies," Report SAND-75-0099, Sandia Laboratories, Albuquerque, NM, June 1975.

19. S. Senderoff, U.S. Patent No. 3,751,298, August 7, 1973.

20. L.G. Boxall, H.L. Jones and R.A. Osteryoung, J. Electrochem. Soc., 121, 212 (1974).

21. R.A. Foust, Jr., "Drybox Purity Control Using Exposed Light Bulb Filament," General Motors Technical Center Letter, Warren, MI, October 3, 1968.

22. D.M. Bush, "Thermal Battery Cell Testing: Apparatus and Results," Report SLA-73-0896, Sandia Laboratories, Albuquerque, NM, December 1973.

23. D.M. Bush, "Results of Thermal Battery Cell Testing," Proceedings 26th Power Sources Symposium, PSC Publications Committee, Red Bank, NJ, 1974, pp 144-147.

24. H.C. Strobel, "Chemical Instrumentation: A Systematic Approach," Addison-Wesley Publishing Company, Reading, MA, 1973, pp 11-13.

25. S.D. James, "Preliminary Study of a Lithium Aluminum Electrode for Thermal Batteries," Report NOL-TR-72-224, Naval Ordnance Laboratory, White Oak, MD, January 1973.

26. S.D. James, Electrochemica Acta, 21, 157 (1976).

27. M. Hansen, "Constitution of Binary Alloys," 2nd Ed., McGraw-Hill Book Co., New York, 1958, pp 104-105.

28. K.M. Myles, F.C. Mrazek, J.A. Smaga and J.L. Settle, "Materials Development in the Li-Al/Metal Sulfide Battery Program at Argonne National Laboratory," Proceedings of the Symposium and Workshop of Advanced Battery Research and Design, Report ANL-76-8, Argonne National Laboratory, Chicago, IL, March 1976, pp B50-B73.

29. D.M. Ryan and L.C. Bricker, "Progress Report: High Energy Density Pelletized Aluminum Chlorine Thermal Batteries - Contract F33615-76-C-2080," Eureka Advanced Science Corp., Bloomington, IL, November 1976.

30. P.V. Clark, "Fused Salt Mixtures: Eutectic Compositions and Melting Points," Report SC-R-68-1680, Sandia Laboratories, Albuquerque, NM, December 1968, p 59.

31. J.C. Nardi, J.K. Erbacher, C.L. Hussey and L.A. King, "Experimental Optimization and Characterization of a $LiAl/NaAlCl_4/MoCl_5$ Pelletized

Thermal Cell," Report SRL-TR-77-0002, F.J. Seiler Research Laboratory (AFSC), USAF Academy, CO, February 1977.

32. W.J. Hamer, "Internal Resistance of Primary Batteries," The Primary Battery, Vol. Two, N.C. Cahoon and G.W. Heise, Ed., John Wiley and Sons, Inc., New York, 1976, pp 430-431.

APPENDIX A

BASIC Program: Constant Current Discharge

Concur 22 Feb 77 Basic/Caps Vol-01

```
1  Rem Constant Current Experimental Battery Discharge Prog
2  Rem Battery OCV not to exceed 5 Volts
3  Rem Programmer = C.L. Hussey  Date = 10 Feb 76
4  Rem
5  Rem
10 Dim A(1000)
20 Print "Battery System?"
21 Input A$
30 Print "Cell Mass (Grams)?"
31 Input W
40 Print "Clock Rate (Sec/Sample)?"
41 Input T
50 Print "Discharge Temperature (Deg-C)?"
51 Input T2
60 Print "Discharge Rate (Amps)?"
61 Input B
70 Print "Cut-off Voltage (Volts)?"
71 Input V1
80 T1 = T*100
81 Rem
82 Rem A/D Conversion of OCV Reading
83 Rem
85 SetR (5,5,100)
90 Wait (0)
100 ADC (O,VO)
105 VO = ((VO-2048)/2048)*5
110 Print
115 Print
116 Print
117 Print "Battery System is: ";A$
118 Print "Open Circuit Voltage I9: ";VO;" Volts"
119 Print
120 Print
125 Print "*****Experimental Battery Discharge Data*****"
126 Print
127 Print
128 Print
129 Print
130 Print "Elapsed Time", "Voltage", "Charge", "Energy Density"
131 Print "(Sec)", "(Volt)", "(Coul)", "(Watt-Hr/lb)"
132 Print
133 SetR (5,5,100)
134 Wait (O)
140 Z=0
141 C=0
142 T4=0
```

```
143 Rem
144 Rem A/D Reading of the Battery Discharge Voltage
145 Rem
150 SetR (5,1,T1)
155 For K=0 To 1000
160 ADC (0,A(K))
165 A(K)=((A(K)-2048)/2048)*5
170 IF A(K)<=V1 Go to 235
175 Led (A(K))
176 Rem
177 Rem Z is the Cum Charge Passed
178 Rem
185 If K=0 Go to 215
186 Z=B*T+Z
190 K1=K-1
195 C=C+(((A(K1)+A(K))/2)*T*B)/60
196 Rem
197 Rem Calculation of Energy Density at Each Voltage Reading
198 Rem
200 Y=(C*453.6)/(60*W)
205 T4=T+T4
210 Go to 220
215 T4=0
216 Y=0
220 Print T4,A(K),Z,Y
225 Wait (O)
230 Next K
235 Print
236 Print
237 Print "Battery System",A$
238 Print "Battery Pellet Weight" ,W,"(Grams)"
240 Print "Open Circuit Voltage" ,VO,"(Volts)"
241 Print "Cut-off Voltage" ,V1, "(Volts)"
242 V2=V0-A(0)
243 Print "IR Drop under Load" ,V2, "(Volts)"
245 Print "Discharge Temperature" ,T2, "(Deg-C)"
250 Print "Discharge Rate" ,B, "(Amps)"
255 Print "Sampling Interval" ,T, "(Secs/Sample)"
260 Print "Total Charge Delivered" ,Z, "(Coul)"
265 Print "Overall Energy Density" ,Y, "(Watt-Hr/lb)"
266 Print
267 Print
268 Print "Discharge Profile"
269 Print
270 Print
271 Rem
272 Rem Ordinate Scaling Based on OCV
273 Rem
275 If V0<1 Go to 300
280 If V0<2 Go to 305
285 If V0<3 Go to 310
290 If V0<4 Go to 315
295 If V0<5 Go to 320
```

```
300 S0=1/60
301 S1=1
302 Go to 330
305 S0=2/60
306 S1=2
307 Go to 330
310 S0=3/60
311 S1=3
312 Go to 330
315 S0=4/60
316 S1=4
317 Go to 330
320 S0=5/60
321 S1=5
322 Go to 330
323 Rem
324 Rem Plotting Routine
325 Rem
330 Print Tab(5); "Scaling Factor is ";S0;"Volts/Div"
332 Print"****I****I****I****I****I****I****I****I****I****I****I"
334 N1=0
335 L=0
336 For J=N1 to 100 Step 10
338 L0=L+J
339 N0=L0
340 X=Int(A(N0)/S0)
342 If N0>=K Go to 400
343 If J=100 Go to 350
346 Print "*";TAB(X);"."
348 Next J
350 C0=L0*T
351 Print "-";C0;Tab(X);"."
352 L=L+100
353 N1=10
361 Go to 336
400 End
```

APPENDIX B

Abbreviated Sample Output: Constant Current Discharge Program

Battery System is: LiAl/C-$CuCl_2$(50-100) at 513 MA at 175
Open Circuit Voltage is: 1.82861 Volts

*****Experimental Battery Discharge Data*****

Elapsed Time (Sec)	Voltage (Volt)	Charge (Coul)	Energy Density (Watt-Hr/lb)
0	1.38428	0	0
3	1.35254	1.539	.089344
6	1.31592	3.078	.176458
9	1.28906	4.617	.261198
12	1.27441	6.156	.345184
15	1.26465	7.695	.428073
18	1.25488	9.234	.510321
21	1.24756	10.773	.592018
24	1.24512	12.312	.673392
27	1.24023	13.851	.754528
30	1.23047	15.39	.835184
⋮			
774	.0292969	397.062	9.80517
777	.0170898	398.601	9.80670
780	9.76563E-03	400.14	9.80757

Battery System	$LiAl/C-CuCl_2$ (50-100) at 513 MA at 175
Battery Pellet Weight	2.97 (Grams)
Open Circuit Voltage	1.82860 (Volts)
Cut-Off Voltage	0 (Volts)
IR Drop Under Load	.512695 (Volts)
Discharge Temperature	175 (Deg-C)
Discharge Rate	.513 (Amps)
Sampling Interval	3 (Secs/Sample)
Total Charge Delivered	400.14 (Coul)
Overall Energy Density	9.80757 (Watt-Hr/lb)

Discharge Profile

Scaling Factor is .0333333 Volts/Div

```
****I****I****I****I****I****I****I****I****I****I****I
*
*
*
*
*
*
*
*
*
*
- 300
*
*
*
*
*
*
*
*
*
*
- 600
*
*
*
*
*
*
*.
Ready
```

APPENDIX C

ENERGY DENSITY CALCULATIONS

Assuming the following reaction of LiAl alloys in the electrolyte:

$$\text{LiAl } (\beta,\gamma, \text{ or } \delta) \xrightleftharpoons{K_D} \text{LiAl } (\alpha+\beta,\beta, \text{ or } \gamma+\delta) + \text{Li}$$

$$3\text{ Li} + \text{NaAlCl}_4 \longrightarrow 3\text{ LiCl} + \text{NaCl} + \text{Al}$$

and that Al is the actual anode in the cell with an open circuit voltage equal to 1.825 ± 0.004 volts at 175°C then for

$$2[\text{Al} + 4\text{NaCl} \rightleftharpoons \text{NaAlCl}_4 + 3\text{Na}^+ + 3\text{e}^-]$$

$$3[\text{CuCl}_2 + 2\text{Na}^+ + 2\text{e}^- \rightleftharpoons \text{Cu} + 2\text{NaCl}]$$

$$2\text{Al} + 2\text{NaCl} + 3\text{CuCl}_2 \longrightarrow 2\text{NaAlCl}_4 + 3\text{Cu}$$

the OCV Energy Density (examples of such calculations are given in the appendix of Reference 13) equals 125.3 W-Hr/lb.

The corrected experimental energy density is given by

$$\text{Corr EED} = (\text{EED}) \frac{\text{Theor. Cell Weight}}{\Sigma \text{ Active Material Weights}}$$

where the theoretical cell weight is usually 3.01 g; the active materials are LiAl in the anode, $CuCl_2$ in the cathode, and NaCl; and the EED is the observed experimental energy density. For Run No. 1008-24, the single cell contained 0.500 g 98.6% pure $CuCl_2$ as the limiting reagent, 0.140 g NaCl was required, 0.270 g 48 a/o LiAl was consumed and the EED was 24.4 W-Hr/lb yielding a Corr EED equal to 80.7 W-Hr/lb. Similar calculations for Run Nos. 1008-22 (60.2 a/o LiAl) and 1008-20 (70.4 a/o LiAl) gave 102.2 and 105.4 W-Hr/lb respectively.

Energy density efficiencies are calculated from the equation

$$\text{Energy Density Efficiency} = \left(\frac{\text{Corr EED}}{\text{OCV Energy Density}}\right)(100)$$

For the data reported in the previous paragraph the energy density

efficiencies were 64.4, 81.6 and 84.1% for the 48, 60.2, and 70.4 a/o LiAl alloys respectively at the 15 mA/cm^2 constant current discharge rate at 175°C.

APPENDIX D

COULOMBIC EFFICIENCY CALCULATIONS

Assuming all the Li in the alloy anode is available by dissociation and that the Al produced by reaction of the Li with the electrolyte is the actual anode, the theoretical charge available for an overall 3 electron oxidation using 0.500 g 48.0 a/o LiAl alloy is:

$$(0.500\text{g LiAl})\left(\frac{0.19\text{ Li}}{1.000\text{g LiAl}}\right)\left(\frac{1\text{ mole}}{6.939\text{g Li}}\right)\left(\frac{1\text{ mole Al}}{3\text{ mole Li}}\right)\left(\frac{3e^-}{\text{mole Al}}\right)\left(\frac{96{,}487\text{ coul}}{e^-}\right)$$

$$= 1321 \text{ coulombs}$$

A similar calculation for the 60.2 and 70.4 a/o LiAl alloys gave 1947 and 2642 coulombs respectively.

The theoretical charge available based on 0.500g 98.6% pure $CuCl_2$ in the cathode for an overall 2 electron reduction is:

$$(0.500\text{g } CuCl_2)(0.986\text{ purity})\left(\frac{1\text{ mole}}{134.45\text{g } CuCl_2}\right)\left(\frac{2e^-}{\text{mole } CuCl_2}\right)\left(\frac{96{,}487\text{ coul}}{e^-}\right)$$

$$= 708 \text{ coulombs}$$

Coulombic efficiencies are given by:

$$\%\text{ Coul Eff.} = \left[\left(\frac{\text{Charge Delivered}}{\text{Theor. Charge Avail.}}\right)\left(\frac{\text{Theor. Cell Wt.}}{\text{Actual Cell Wt.}}\right)(100)\right]$$

where the theoretical charge available is 708 coulombs and the theoretical cell weight is 3.01g. The data for the 3 LiAl alloys is reported in Table D1.

Table D1: Coulombic Efficiencies for $LiAl/NaAlCl_4/CuCl_2$ Cells at 15 mA/cm^2 at 175°C

Run No.	LiAl (a/o)	Charge Delivered (Coul)	Actual Cell Wt (g)	% Coul Eff.[a]
1008-24	48	655	2.985	93.3
1008-22	60.2	670	2.995	95.1
1008-20	70.4	680	2.970	98.0

[a] $\%\text{ Coul Eff.} = \left(\frac{\text{Charge Delivered}}{708\text{ Coul}}\right)\left(\frac{3.01\text{ g}}{\text{Actual Cell Wt}}\right)(100)$

ATE

LMED

-7

CONT

AD-A045 620 FRANK J SEILER RESEARCH LAB UNITED STATES AIR FORCE --ETC F/G 10/3
THE DISCHARGE BEHAVIOR OF A LIAL/NAALCL4/CUCL2 PELLETIZED THERM--ETC(U)
FEB 77 J K ERBACHER, C L HUSSEY, L A KING
UNCLASSIFIED FJSRL-TR-77-0001 NL

2 OF 2
AD
A045620

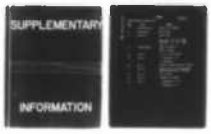

END
DATE
FILMED
1 -78
DDC

SUPPLEMENTARY

INFORMATION

AD-A045620

045620

ERRATA

FJSRL-TR-77-0001, February 1977.

Page	Item	Change
v	Title Table VIII	delete "s" in Voltages
9	superscript d	AlCl to $AlCl_3$
12	Equation 4	should read: $\frac{\sigma_{EED}}{EED} = \left[\frac{\sigma_i^2}{i^2} + \frac{\sigma_\varepsilon^2}{\varepsilon^2} + \frac{\sigma_t^2}{t^2} + \frac{\sigma_w^2}{w^2}\right]^{\frac{1}{2}}$
14	Column Heading	"COV^d: 0.8 Volts" to "COV^d: 1.0 Volts"
29	line 15	"α" to "γ" in two places
32	line 18	"...$CuCl_2$/LiAl..." to "...LiAl/$CuCl_2$..."
43	Ref. 2	"Hesse" to "Heise" and "Ed." to "Eds."
45	Ref. 28	second "of" to "on" and add closing quotation marks after "...Design,"
46	Ref. 32	"Ed." to "Eds."
51	line 3	"1.82860" to "1.82861"
52	line 12	"...Reference 13..." to "...Reference 12..."

ATE
LME